# High-Performance Braces for Seismic Design

By

Tim S. Lim

B.E. Civil Engineering

The Cooper Union for the Advancement of Science and Art, 2012

Submitted to the Department of Civil and Environmental Engineering

in Partial Fulfillment of the Requirements for the Degree of

MASTER OF ENGINEERING IN CIVIL AND ENVIRONMENTAL ENGINEERING

at the

MASSACHUSETTS INSTITUTE OF TECHNOLOGY

JUNE 2013



Signature of Author: _____

Department of Civil and Environmental Engineering
May 10, 2013

Certified by: _____

Jerome J. Connor
Professor of Civil and Environmental Engineering
Thesis Supervisor

Accepted by: _____

Heidi M. Nepf
Chair, Departmental Committee for Graduate Students

# High-Performance Braces for Seismic Design

By

Tim S. Lim

Submitted to the Department of Civil and Environmental Engineering
on May 10, 2013 in Partial Fulfillment of the Requirements for the Degree of
Master of Engineering in Civil and Environmental Engineering

**ABSTRACT**

The fundamental challenge for the structural engineer in designing earthquake-resistant structures is to design buildings with both adequate ductility and sufficient stiffness. Traditional lateral force resisting systems such as the moment resisting frame and the concentrically braced frame are both conventional structural schemes that have been implemented for many years, but result in only mediocre performance levels. The lacking stiffness of a moment resisting frame as well as the limited ductility of a concentrically braced frame gave impetus for engineers to direct significant research efforts into the development of new lateral resisting systems that embody a more stable hysteretic behavior, adequate ductility, control of damage, and energy dissipating capacity.

Fortunately, several recent developments have allowed engineers to move one step closer to designing more efficient earthquake-resistant structures. "High-performance braces," as this thesis calls them, are new and improved bracing systems that combine the economy and stiffness of a concentrically braced frame with the ductility and energy dissipating capacity of a moment resisting frame.

This thesis analyzes and evaluates three different types of high-performance braces: (*i)* the buckling-restrained brace frame, (*ii*) the self-centering energy dissipating brace frame, and (iii) the hybrid brace frame, with regards to their structural performance and economy. The primary goal of the thesis is to provide useful insights into the current developments of high-performance braces for practicing engineers in the hope that such systems can be more widely adopted and utilized in the contemporary design of earthquake-resistant structures.

*Keywords: High-performance braces, earthquake-resistant structures, seismic design*

Thesis Supervisor: Professor Jerome J. Connor
Title: Professor of Civil and Environmental Engineering

**ACKNOWLEDGMENTS**

First and foremost, I want to extend a deep, personal gratitude to Professor Jerome J. Connor for his guidance and support throughout my time here at MIT. His dedication to the students and their learning is truly unsurpassed. I cannot be more grateful for his sharing of knowledge and passion for the profession. All of us here are very lucky to have had the opportunity to be mentored by Dr. Connor.

Second, I must thank all of my peers in the program, whose friendship and kindness have given me great joy throughout the whole year. It was truly an honor and a pleasure to work and grow alongside them.

I also want to express sincere gratitude to my parents as well as my brother for their unflagging support in all aspects of my life. Lastly, I must thank my fiancé, whose love and encouragement have brought me this far and continue to inspire me to live out my dreams.

# Contents

# List of Figures

# List of Tables

# Chapter 1

# Introduction

*"Engineering problems are under-defined, there are many solutions, good, bad and indifferent. The art is to arrive at a good solution. This is a creative activity, involving imagination, intuition and deliberate choice." – Sir Ove Arup*

## 1.1 Background

The main job of the structural engineer is to ensure public trust in the safety of the built environment. Not only is it fundamentally critical to design structures that safely and reliably provide shelter for people, but it is also the aim of the engineer to strive for economy, architectural appeal, and structural performance through the design.

In regions of high seismic risk, there is the additional challenge of building structures to resist and weather such extreme natural disasters. The field of structural engineering has

evolved quite significantly over the past several decades in its approach to designing earthquake-resistant structures. While it always has been and will remain the foremost intent of seismic codes to prevent sudden collapse and failure of structures under extreme events, the impetus for the field to come up with solutions that are more optimized and efficient has been markedly realized in recent years.

Performance-based design is an all-encompassing term used to describe the method in which the design criteria is based on achieving certain performance goals under various levels of seismic hazards. These performance goals may refer to criteria such as the lateral floor displacements, peak floor accelerations, or a target damage state of the building as a result of an earthquake. Although performance-based design and its adoption in contemporary practice have proved useful and enabled increased reliability of the expected structural performance of buildings under seismic events, the ever increasing demand for optimization of the performance of structures in order to minimize the level of damage, economic loss, and repair costs will continue to push engineers to come up with better solutions.

There are two overarching performance objectives in designing efficient earthquake-resisting steel structures: (*i*) adequate lateral stiffness to limit large displacements during elastic response to minor and moderate earthquakes, and (*ii*) sufficient ductility to withstand large inelastic displacements under extreme earthquakes and prevent sudden collapse. The challenge of optimizing the seismic performance of structures lies in the balance of these two parameters, stiffness and ductility.

The most conventional and prevalent lateral force resisting systems utilized in buildings designed for earthquakes are the moment resisting frames (MRFs) and the concentric braced frames (CBFs). In general, CBFs are considered as a more efficient system than the MRFs due to several factors including the structural advantage of taking loads by axial action of the braces rather than through the bending action of the beams and columns in a MRF. Furthermore, the weight of the steel frame, which can directly affect cost, can be significantly reduced by utilizing a CBF system over a MRF.

However, CBFs possess an inherent flaw in that this conventional bracing scheme lacks adequate ductility, and in turn, has a limited energy dissipation capacity. During extreme seismic events, the energy associated with the earthquake causes buckling of the braces and

large inelastic deformations in the brace end connections. Research has shown that this post-yield deformation actually occurs at relatively moderate story drifts, well below the limit states as prescribed by standard codes. On the other hand, MRFs with proper detailing provide sufficient ductility to dissipate energy under extreme seismic events, but require heavy and expensive steel sections for adequate stiffness.

In order to address the issue of limited ductility in conventional CBFs, significant research efforts have been directed towards the development of new CBF systems with a more stable hysteretic behavior, adequate ductility, ability to control damage, and greater energy dissipation capacities. Due to this increased interest in research, there have been several key advancements in the field of brace systems for seismic design in recent years, providing both stiffness and ductility in one single brace system. The term, "high-performance braces," as used in this thesis, refers to these new and improved brace systems.

## 1.2 Scope of Research

The high-performance brace systems this thesis will mainly focus on are the (*i*) buckling-restrained brace frames (BRBFs), (*ii*) self-centering energy dissipating brace frames (SCEDs), and (*iii)* hybrid brace frames (HPCDs). The research will aim to evaluate and compare these various high-performance brace systems with regard to structural performance and economy. The primary goal of the thesis was to provide useful insights into the current developments of high-performance braces in the hope that such systems can be more widely adopted and utilized by practicing engineers in designing new earthquake-resistant structures.

After providing a comprehensive overview on the breadth of available literature regarding high-performance braces, the thesis will present the methodology in developing analysis models used to evaluate the structural performance of the various systems. The structural analysis will be performed using the Computers and Structures, Inc. (CSI) program SAP2000. A comparative analysis will follow that will highlight the various performance levels of the three different types of high-performance braces. Following these results, a discussion of the performance implications as well as a parallel evaluation of the economic aspects of these new systems will be presented. The thesis will then conclude with final remarks and recommendations for future research.

# Chapter 2

# Literature Review

The following chapter provides an overview of the available research on the topic of high-performance braces. For each type of brace system: BRBF, SCED, and HPCD, the chapter will present the background and its current practices, the high-performance aspects, then the design methods, mathematical formulations and modeling considerations, in that respective order. The background outlined in this review will serve as the basis for discussion in subsequent chapters.

## 2.1 Buckling-Restrained Braces

### *2.1.1 Background and Current Practice*

The concept of using yielding steel elements in structural systems to dissipate energy in seismic events was first introduced in 1975 through research done at the New Zealand

Society for Earthquake Engineering (Skinner et al., 1975). Due to the distinctive ability for steel members with known yield strengths to undergo inelastic deformations at expected capacities led to the development of using this ductile behavior of the material to work as a hysteretic damper in systems. Utilizing the ductility of steel members and their capability of performing beyond the elastic limit repeatedly in cyclic loadings form the basis for seismic energy dissipation.

In 1971, researchers Yoshino and Karino of the Architectural Institute of Japan introduced a refined brace concept in the form of "Shear Wall with Braces" (Yoshino & Karino, 1971). This novel notion of restraining the buckling behavior of the steel braces in compression by encasing the member in concrete was the first direct inspiration for the eventual conceptualization of the BRB. Expanding on this idea of buckling-restraint through encasement, Kimura and others developed the first working concept of conventional steel braces encased in mortar-filled steel tubes in 1976 (Kimura et al., 1976).

Since then, multiple experiments have been conducted in the laboratory to test the reliability of the desired hysteretic behavior of these new devices. However, findings showed that under subsequent cycles of loading, the braces failed due to the transverse deformation of the mortar allowed for local buckling of the steel element within the encasement. Data showed that approximately 10-15% of the longitudinal strains of the core were transferred to the restraining encasement. The coupled action of the transverse shear deformation between the steel core and the encasement was only mitigated by the breakthrough development of the "unbonded brace," as coined by the Nippon Steel Corporation in 1988.

The first original and proprietary BRB concept available for commercial application was introduced by Nippon Steel Corp in the late 1980s. The company commissioned several research projects in order to validate the effectiveness of this new high-performance brace. Full decoupling of the yielding steel core element and the mortar-filled encasement was the key advancement that allowed for the desired performance of the concept of the BRB.

The adoption of BRBs gained traction immediately in Japan, where seismic risk is of high concern for engineers. As early as the late 1980s, BRBFs have been implemented in several different types of structures, and continued to proliferate to hundreds of applications by the

1990s. As illustrated in the figure below, BRBF systems has a significant market share in structural systems utilized for high rises built in Japan from 1995 to 1999.

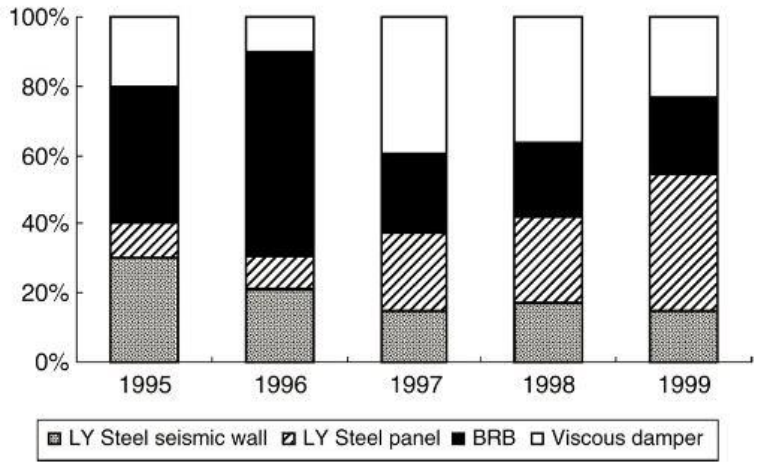


Figure 2.1-1: BRB Use in High Rise Buildings in Japan from 1995-1999

The entry to market in the United States was not immediate and began only in 1999, when experimental tests were conducted at the University of California, Berkeley as qualification for installation in two new buildings being constructed in the region (Black et al., 2004). Since then however, the adoption in the United States and other areas outside Japan such as Canada and parts of Europe, has been on the rise, at least in high seismic zones.

Due to the nature of BRBs being essentially a refined concept of the conventional CBF, practical implementation did not require very different design approaches. The CBF system has been widely utilized in different styles of structures ranging from low-rise warehouses to high-rise office towers, as well as everything in between. Therefore, the adaptation of the use of high-performance braces in practice was relatively swift (Tinker, 2011).

### *2.1.2 High-Performance Aspects*

A schematic and a typical longitudinal section view of a typical BRB element has been illustrated below to form the basis for discussion of the details of the brace.

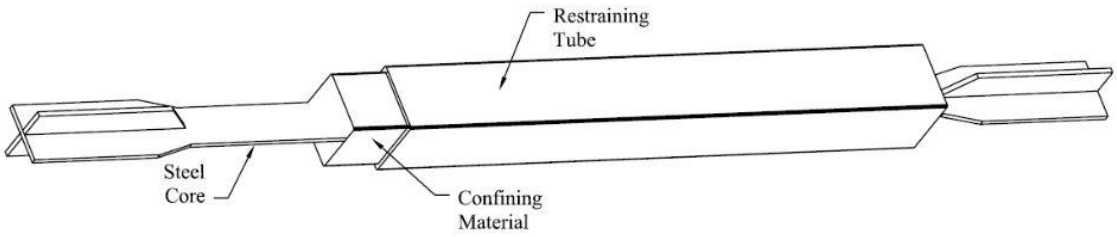


Figure 2.1-2: Schematic of a Typical BRB

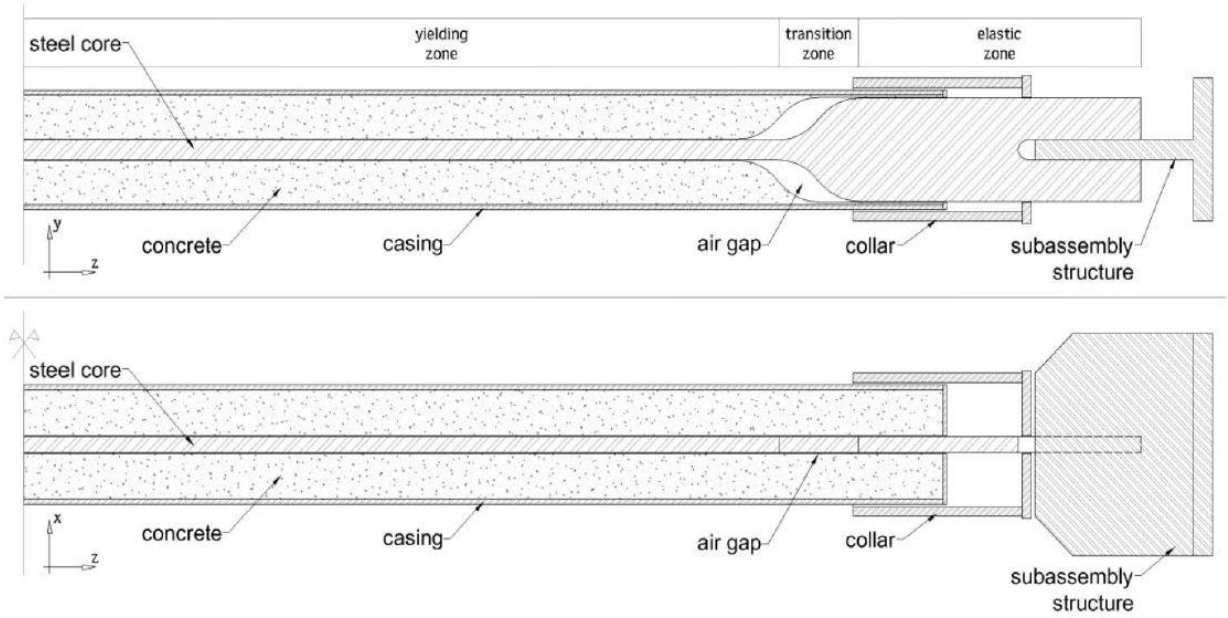


Figure 2.1-3: Typical Longitudinal Section of BRB

As previously delineated in the preceding section, the BRB is a refinement to the conventional steel brace, comprising of an inner steel core encased in a mortar-filled case that restrains the yielding steel from buckling under compression. The interacting surface between the steel core and the confining material is coated with an unbonding agent to effectively decouple the transverse deformations of the two subsystems. When concrete is employed as the encasement material, several types of unbonding materials are available for use, such as epoxy resin, silicon resin, and vinyl tapes (Xie, 2004). Further research into the unbonding material has looked into even more options such as silicon coating, styrofoam, polyethylene films, and butyl rubber sheets. An idealized model illustrating the decoupled system of the BRB is shown below.

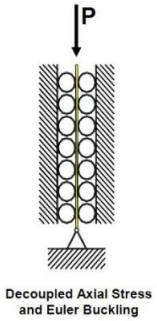


Figure 2.1-4: Idealized BRB Behavior under Axial Load (Hussain, 2005)

The rather simple but immensely profound advantage of BRBs over conventional steel braces is that this high-performance brace exhibits the same behavior in both tension and compression. The figure below shows the balanced hysteretic behavior of the BRB in both tension and compression, highlighting the limitations of the conventional braces under compressive loadings.

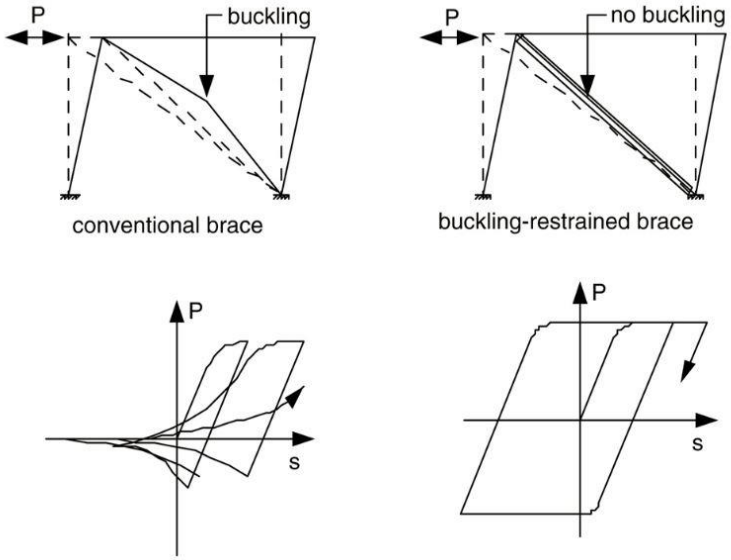


Figure 2.1-5: Behavior of CBF vs. BRBF under Cyclic Loadings (Xie, 2004)

There are several different configurations of BRBs that exist, which vary in cross-sections of the steel core elements. As shown in Figure 2.1-6 below, cross-sections can vary from flat plates, wide-flanges, and even HSS round sections.

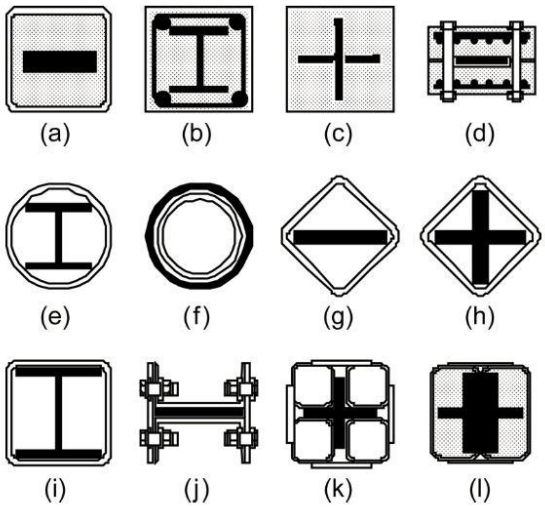


Figure 2.1-6: Typical Cross-Section Configurations of BRBs (Xie, 2004)

The illustrated configurations show different combinations of varying types of steel core and the restraining jacket. Configurations (a) through (c) are mortar-filled BRBs, (d) is a bolted precast concrete restraint, and (e) through (l) are fully steel BRBs.

As emphasized before, the decoupling of the core steel brace element with the buckling-restraining encasement is of critical importance. The yielding steel core must be able to slide freely inside the casing so that the transverse expansion of the brace can occur in an unimpeded manner.

### *2.1.3 Design Methods, Mathematical Formulation, and Modeling Considerations*

The development of high-performance braces, BRBs in particular, served as an impetus in driving building codes to adopt new technologies in seismic standards in response to the advancements in structural performance these systems offer. The BRBF system is included in the *American Institute of Steel Construction (AISC) Seismic Provisions for Structural Steel Buildings 2005*, which is adopted by reference in both the *International Building Code 2006* and the *California Building Code 2007*. Furthermore, the *ASCE 7-05: Minimum Design Loads for Buildings and Other Structure* also formally adopted the BRBF system as a legitimate seismic-resisting structural system.

There is a limitation, however, to the pertinent codes for BRBFs in that the current provisions are mostly prescriptive requirements with appropriate overdesign factors accounting for the

strength of BRB connections that compensate for the unforeseeable possibility of the failure of components not expected to exceed their elastic limit such as beams, columns, gusset plates, and connections. The *AISC Seismic Provisions* claims unavailability of sufficient test data for such prescriptive requirements, but as additional tests and case studies of BRBFs become readily available in the United States, the codes will become more accurate and reliable.

As explained previously in the background section, the ductility of a lateral force resisting system dictates the magnitude of its response to seismic excitations. The seismic codes measure the ductility of different types of lateral systems with the Response Modification Coefficient (R), with higher values corresponding to more ductile systems. The table below outlines the entire ductility spectrum of many different types of lateral systems as per the seismic codes pertinent to buildings in the United States.

| **Comparison of Typical Lateral Force Resisting Systems** | | |
|---|---|---|
| **System** | **Response Modification Coefficient (R)** | **Deflection Amplification Factor ($C_d$)** |
| Ordinary Moment Frames (OMF) | 3.5 | 3 |
| Intermediate Moment Frames (IMF) | 4.5 | 4 |
| Special Concentrically Braced Frames (SCBF) | 6 | 5 |
| Eccentrically Braced Frames (EBF) | 7 | 4 |
| Special Plate Shear Walls (SPSW) | 7 | 6 |
| Buckling-Restrained Braced Frames (BRBF) | 7 | 5.5 |
| Special Moment Frames (SMF) | 8 | 5.5 |

Table 2.1-1: Ductility Comparison of Typical Lateral Systems (ASCE/SEI 7-10)

The BRBF's ductility is in the higher end of the spectrum, near that of the SMF, which is a testament to the effectiveness of this high-performance brace. The BRBF possess similar levels of stiffness in controlling lateral displacements with that of the CBF, all the while having the ductile capacity nearing that of the SMF to withstand large inelastic deformations under extreme seismic events.

The basis for acceptable design of BRBs as per code is driven by the "adjusted brace strength," which accounts for the overdesign of the strength of BRB connections as described above. In the *AISC Provisions,* the process of designing adequate BRBs is as follows:

$$P_{ysc} = F_{ysc} \cdot A_{sc} \tag{1}$$

$$P_u = \varphi \cdot \beta \cdot \omega \cdot R_y \cdot P_{ysc} \tag{2}$$

$$P_u = \varphi \cdot \omega \cdot R_y \cdot P_{ysc} \tag{3}$$

Firstly, the brace design axial strength ($P_{ysc}$) is calculated by multiplying the minimum yield stress of the core element ($F_{ysc}$) by the net area of the steel core ($A_{sc}$) as shown in Equation (1). Equations (2) and (3) are the compressive and tension force capacities of the brace, respectively. The compression strength adjustment factor ($\beta$) is the code provided factor to account for BRB's compression overstrength. Lastly, the material expected yield stress ($R_y$) and the strain hardening factor ($\omega$) also factor in the brace's design capacity. The design process of BRBFs as per the *AISC Provisions* is best summarized by the follow flowchart.

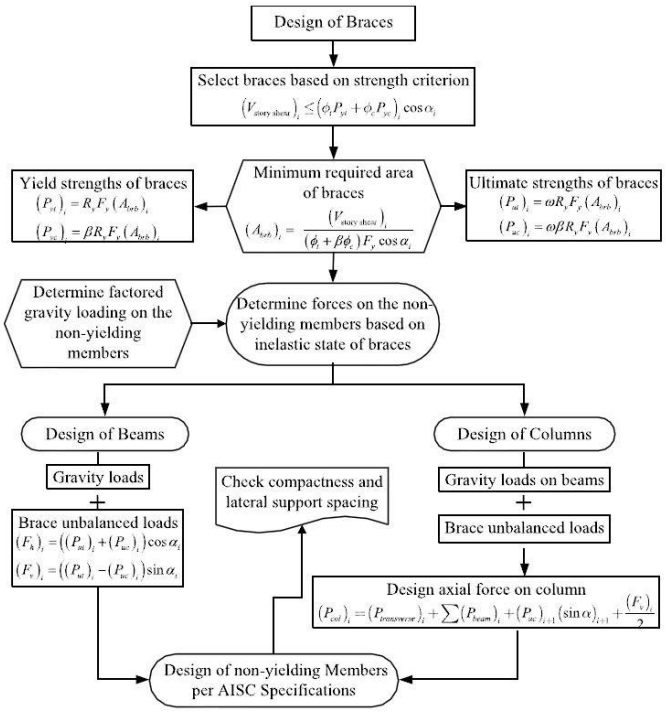


Figure 2.1-7: Flowchart for BRBF Design as per AISC Provisions (Dipti, 2010)

Due to the lack of any empirically based equations for the design of BRBs, researchers have presented various mathematical models of the BRB element, based on the available qualification test data (Tinker 2011). Since the design of the buckling-restrained brace involves the need to investigate all potential ways for instabilities to form in the compression regime, the modeling is divided into three distinct modes of buckling: (*i*) global flexural buckling of the entire brace, (*ii*) local buckling of the core element outstands, and (*iii*) plastic torsional buckling of the unrestrained core ends.

The global buckling mathematical model for a composite BRB, in which the yielding core is a steel bar encased by a reinforced concrete material, is formulated and analytically expressed in the following section (Xie, 2005). The figures below illustrate the variables used in the formulation.

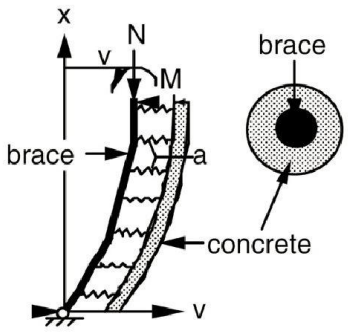


Figure 2.1-8: Composite BRB - Forces in the System

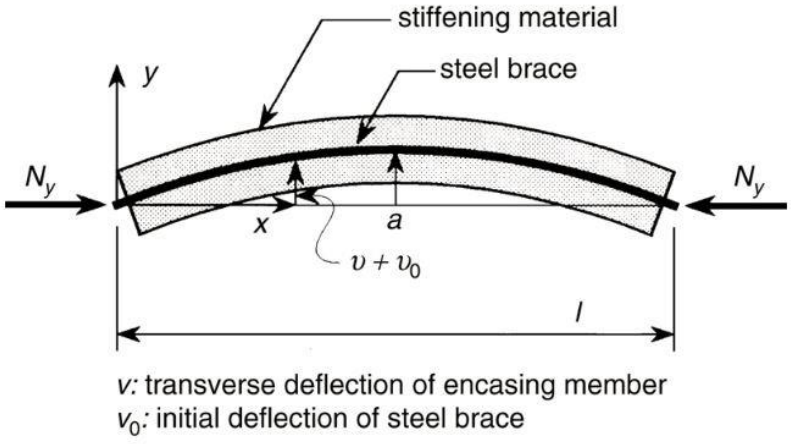


Figure 2.1-9: Composite BRB - Transverse Deflection of Brace

As shown in Figure 2.1-8, the brace has a deformation expressed as:

$$v = \delta \ sin\frac{n\pi x}{l} \tag{4}$$

in which, $v$ is the deflection of the encasing concrete, and $\delta$ is the deflection in the midspan. Assuming that the deformations in the steel brace and the concrete encasement are the same, the distributed lateral force in Equation (4) can be written as:

$$p = \frac{n^4\pi^4}{l^4}\delta E_C I_C \ sin\frac{n\pi x}{l} \tag{5}$$

where $E_C I_C$ is the flexural stiffness of the concrete. Diving (5) by (4), the following expression is obtained:

$$\alpha = \frac{p}{v} = \frac{n^4\pi^4}{l^4}E_C I_C \tag{6}$$

In Equation (6), α is defined as a resistant coefficient, representing the required force distribution per unit deflection of the concrete encasement, similar to the spring constant.

Since the deformation of the core steel brace is restrained by the encasing concrete, the bending moment is as follows:

$$M(x) = -Rx + \int_0^x \alpha v \cdot x \cdot dx + Nv \tag{7}$$

where, $M(x)$ is the bending moment at the cross-section, $R$ is the reaction at the hinge, $x$ is the distance from the hinge to the cross-section, and $N$ is the axial force.

From (7), the Euler differential equation can be obtained:

$$\frac{d^4v}{dx^4} + k^2\frac{d^2v}{dx^2} + \beta v = 0 \tag{8}$$

in which, $k^2 = \frac{N}{E_S I_S}$ and $\beta = \frac{\alpha}{E_S I_S}$.

Taking the boundary conditions such that both ends are assumed to be perfect pin connections, the following two expressions are obtained:

$$N^2 = 4\alpha E_S I_S \tag{9}$$

$$N_{cr} = \frac{2n^2\pi^2 E_S I_S}{l^2} \tag{10}$$

Using (9) and (10), the buckling mode length can be obtained:

$$\frac{l}{n} = \pi\sqrt{\frac{E_S I_S}{\alpha}} \tag{11}$$

Combining (10) and (11), the critical axial load can be divided into two parts:

$$N_{cr} = \frac{n^2\pi^2 E_S I_S}{l^2} + \frac{l^2}{n^2\pi^2}\alpha \tag{12}$$

where the second part in the expression in (12) represents the contribution of the encasement to the buckling limit.

Substituting (6) into (12), the total buckling load can be obtained:

$$N_{cr} = \frac{n^2\pi^2}{l^2}[E_S I_S + E_C I_C] \tag{13}$$

Notice that the total buckling load expression is a simple sum of the contributions of the two separate parts in the composite BRB specimen. However, to better model realistically manufactured BRBs, the degradation of the concrete stiffness due to imperfect unbonding agents must be considered, as in the next formulation:

$$N_{cr} = \frac{\pi^2}{l^2}[E_S I_S + kE_B I_B] \tag{14}$$

The $k$ factor which ranges from 0 to 1 represents the stiffness degradation in the concrete encasement, and $E_C I_C$ is also rewritten as $E_B I_B$.

Assuming $E_S = 0$ after the steel core member yields, the necessary stiffness of the concrete encasement can be obtained as follows:

$$\frac{\pi^2}{l^2} kE_B I_B \geq N_y \tag{15}$$

The stiffness and strength of the encasement are coupled parameters that need to be determined in order design BRBs for desirable behavior of symmetric yielding action on both tension and compression regimes. A highly stiff encasement with low strength will not

provide adequate stiffening behavior desired in BRBs once the encasement is cracked or damaged, and inversely, a high strength low stiffness encasement will not provide enough restraint to stop the steel brace from buckling.

To address this coupling behavior between the stiffness and strength of the encasement, suppose the brace yields without buckling under axial compression force, as shown in Figure 2.1.3-2. The initial deflection is then defined as:

$$v_0 = a \sin\frac{\pi x}{l} \tag{16}$$

where $v_0$ is the initial deflection and $a$ is the initial deflection of the midspan. At this point, an equilibrium can be obtained in the brace:

$$E_B I_B \frac{d^2 v}{dx^2} + (v + v_0) N_y = 0 \tag{17}$$

for which $E_B I_B$ is the flexural stiffness of the encasing member. The transverse deflection of the encasement can then be obtained as a general solution to the differential equation above:

$$(v + v_0) = \frac{a}{1 - \frac{N_y}{N_E^B}} \sin\frac{\pi x}{l} \tag{18}$$

where,

$$N_E^B = \frac{\pi^2 E_B I_B}{l^2} \tag{19}$$

The term $N_E^B$ is the Euler buckling load of the encasing member, and from (19), the bending moment at the midspan of the member can be obtained:

$$M_C^B = \frac{N_y a}{1 - \frac{N_y}{N_E^B}} \tag{20}$$

For a particular case when a square steel tube is employed as the encasement, the maximum stress $\sigma_k$ in the outermost fiber of the tube can be obtained:

$$\sigma_k = \frac{N_E^B \cdot N_y}{N_E^B - N_y} \cdot a \cdot \frac{D}{2I_B} \tag{21}$$

where, $D$ and $I_B$ are the depth and moment of inertia of the encasement, respectively.

With regards to strength, the maximum stress cannot exceed the yielding stress of the encasement, $\sigma_k < \sigma_{ky}$. Therefore, the stiffness and strength requirements for the encasement can be obtained as follows:

$$\frac{N_E^B}{N_y} > 1 + \frac{\frac{\pi^2 E_B \cdot \frac{a}{l_B}}{2\sigma_{ky}}}{\frac{l_B}{D}} \tag{22}$$

for which, $\sigma_{ky}$ and $l_B$ are the yielding stress and length of the steel tube respectively. More generally, by defining $M_y^B$ as the yielding moment of the encasing member, which is the limiting bending moment in the member to sustain flexural stiffness $E_B I_B$, then the stiffness criterion is as follows:

$$M_C^B < M_y^B \tag{23}$$

Setting two new terms $n_E^B, m_y^B$ as:

$$n_E^B = \frac{N_E^B}{N_y}, m_y^B = \frac{M_y^B}{N_y l} \tag{24}$$

and combining (20) with (23), the global buckling criterion can be expressed as:

$$\left(1 - \frac{1}{n_E^B}\right) m_y^B > \frac{a}{l} \tag{25}$$

## 2.2 Self-Centering Energy Dissipating Braces

### *2.2.1 Background and Current Practice*

The self-centering energy dissipating brace (SCED) is another type of high-performance brace that builds on the concept of the BRB, but with the added ability to "self-center" itself through the utilization of shape memory alloys, which in turn minimizes residual drifts in the structure after minor or moderate earthquakes. The SCED is comprised of a main re-centering component, made of pre-tensioned superelastic NiTi shape memory alloy (SMA) rods, also known as Nitinol, and a passive energy dissipation mechanism through friction pads clamped together with tensioned bolts.

Although the BRBF, as presented in the previous section, possesses numerous desirable performance benefits over a traditional CBF, it is prone to residual lateral deformations of damage concentration over the building height unless it is backed up by a more ductile secondary lateral system such as the MRF (Tremblay et al., 2003). Large residual deformations in a building after a strong earthquake can make the structure appear unsafe to occupants, impair significant structural damage and thus its response to subsequent aftershock earthquakes, and significantly increase the cost of postseismic repair or replacement (Zhu and Zhang, 2008). Furthermore, residual deformations are emphasized as a fundamental complementary parameter in evaluating both structural and non-structural damage in buildings that are based on performance-based design criteria (Pampanin et al., 2003). Therefore, the development of a system that can return to its initial position after an earthquake, all the while still possessing many of the characteristics of a high-performance BRBF, has attracted considerable amount of attention in the field (Miller et al., 2011).

The use of smart metallic materials such as Nitinol and other SMAs as an energy dissipation mechanism has been around in the medicine and aerospace industries for quite some time (Bank and Weres, 1976, Chandra et al., 2001). The alloy's inherently unique ability to fully recover at the end of a deformation process, either spontaneously (superelastic effect) or through a heating treatment (shape memory alloy effect) has made it possible for researchers to tinker with the concept of applying self-centering properties to other mechanisms. However, Dolce et al. (2000) were the first to apply SMAs in structures, employing the properties of Nitinol wires to conceive, design, manufacture, and test several self-centering bracing devices for seismic protection of buildings (Dolce et al., 2000). Since then, considerable research has been conducted in trying to optimize the implementation of these SMA energy dissipating mechanisms. It is important to note that in general, the use of shape memory alloys as damper systems are expensive to construct and do not scale easily to all ranges of design forces (Christopoulos et al., 2008). A further evaluation of the economic practicality as well as the scalability of the performance of SCEDs will be presented in later chapters.

### *2.2.2 High-Performance Aspects*

A conceptual illustration of a typical SCED brace element, as developed by Christopoulos et al. (2008) is shown below in Figure 2.2-1. The system consists of a tensioning system and an

energy dissipation system, both connected by a series of guiding elements. The abutting element is configured and sized to interact with the tensioning system on both ends of the two structural elements. Lastly, a dissipative mechanism, via the friction device, is connected to the two bracing members and is only activated when relative motion is induced between these two members (Christopoulos et al., 2008).

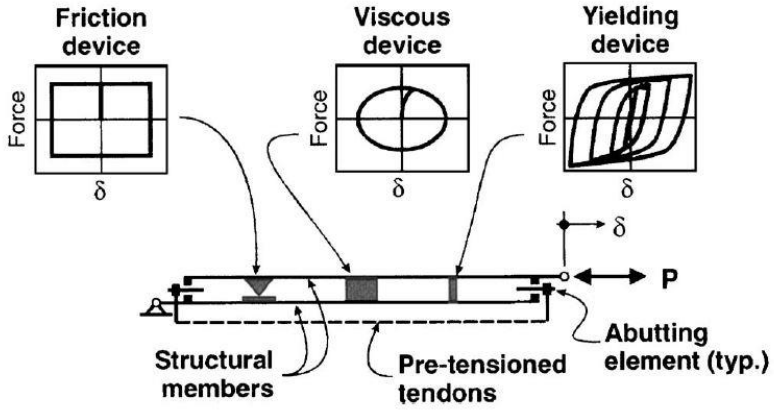


Figure 2.2-1: Concept of SCED System (Christopoulos et al., 2008)

The number of tensioning elements and their corresponding modulus of elasticity, initial pretensioning force, ultimate elongation capacity, total area, and length are all design parameters that determine the strength, post-elastic stiffness, deformation capacity, and self-centering capacity of the SCED system. The pretension force in the tensioning system determines the force level at which the relative movement starts between the two structural elements. Therefore, the assemblage of the system can be designed such that when relative motion is induced, it always results in the elongation of the tensioning elements. This elongation activates the energy dissipation mechanism, and therefore, changes the effective stiffness of the system from the initial elastic stiffness, as determined by the sum of the two structural elements, to the post-elastic stiffness, determined now by the stiffness of the tensioning elements.

The behavior of an idealized SCED brace element and its desirable flag-shaped hysteretic response is illustrated in the figure below. The four diagrams represent the deformation behavior of the SCED for four different loading stages: (a) the force *P* has not overcome the pretensioning force, and therefore, the brace element shows a high initial axial stiffness, (b) the force *P* has overcome the pretensioning force and has activated the post-elastic stiffness

of the tensioning element and the energy dissipation mechanism, and in turn, increasing the tension in the elements to provide a positive restoring force to the system, (c) the self-centering property is shown in the system as the tension in the elements is larger than the force necessary to activate the dissipation mechanism, and (d) the reversed action is shown.

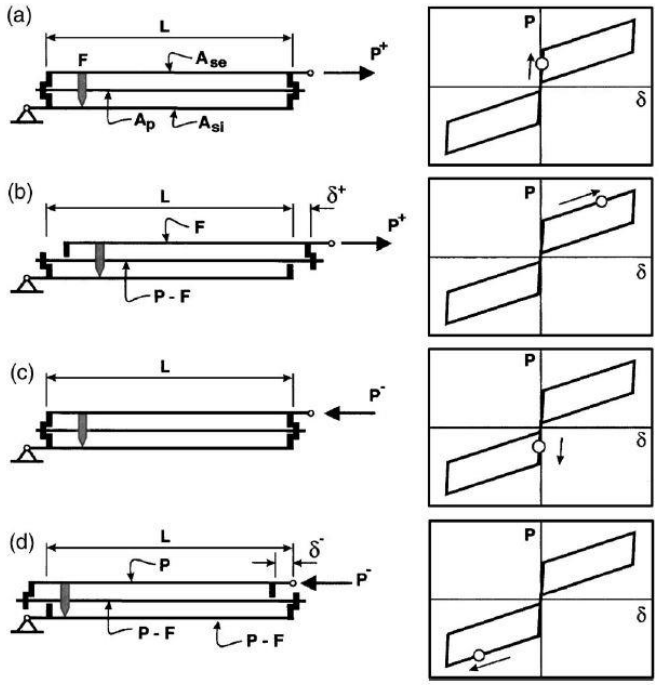


Figure 2.2-2: Mechanics and Hysteretic Response of SCED Systems (Christopoulous et al, 2008)

In conclusion, the flag-shaped hysteretic behavior of the SCED can be simply summarized by the following diagram, illustrating the contributions of the two components that make up the SCED.

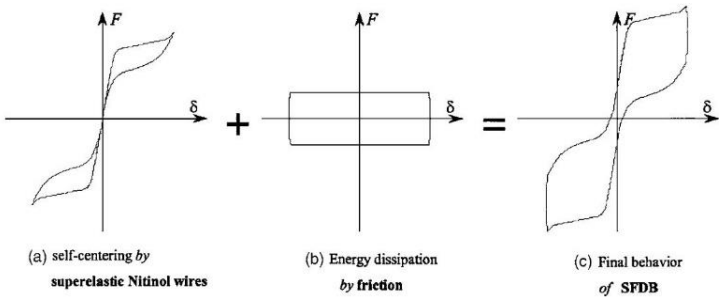


Figure 2.2-3: Flag-Shaped Hysteretic Behavior of SCED (Zhu and Zhang, 2008)

### *2.2.3 Design Methods, Mathematical Formulation, and Modeling Considerations*

As emphasized in the previous section, the design of SCED systems is governed by many parameters such as the number of tensioning elements and their corresponding modulus of elasticity, initial pretensioning force, ultimate elongation capacity, total area, and length. To determine the strength, post-elastic stiffness, deformation capacity, and self-centering capacity of the SCED system, it is important to explicitly model the behavior of the SCED brace element as a function of the design parameters.

The formulation of the response of the SCED element as delineated by Christopoulous et al. (2008) is based on the schematic shown below.

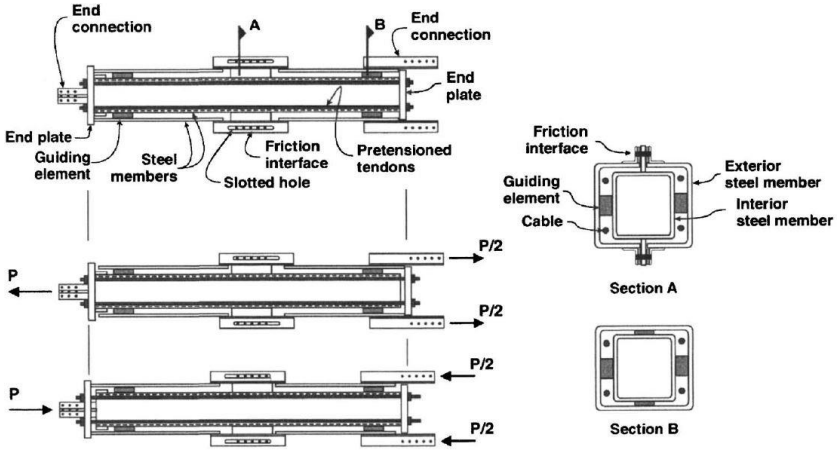


Figure 2.2-4: Embodiment of SCED Element (Christopoulous et al., 2008)

The frictional resistance of the energy dissipation mechanism is denoted as $F$ and the initial tendon pretension is labeled as $T_{p0}$. At rest, the pretension force $T_{p0}$ applies compressive forces $P_{si,0}$ and $P_{se,0}$ to the interior and exterior steel members, respectively. These initial forces are relative to the axial stiffness of each member by the following expressions:

$$P_{si,0} = \frac{T_{p0}K_{si}}{K_{si}+K_{se}} \; ; \; P_{se,0} = \frac{T_{p0}K_{se}}{K_{si}+K_{se}} \tag{26}$$

where, $K_{si}$ and $K_{se}$ are axial stiffness of the interior and exterior steel members, respectively. The relative movement between the two members initiates when the load applied to the SCED brace element reaches the activation load as expressed:

$$P_a = F + T_{p0} + K_p\delta_a \tag{27}$$

for which, $K_p$ is the axial stiffness of the tendons as given by $K_p = \frac{E_s A_s}{L}$, and $\delta_a$ is the deformation of the brace at the onset of activation. Prior to activation of the system, the elastic stiffness of the brace can be expressed as:

$$K_{be} = K_{si} + K_{se} + K_p \tag{28}$$

Since the deformation of the brace can also be expressed as:

$$\delta_a = \frac{P_a}{K_{be}} \tag{29}$$

the activation force $P_a$ can be rewritten by substituting (29) into (27):

$$P_a = \frac{F + T_{p0}}{1 - \frac{1}{K_{be}}} \approx F + T_{p0} \tag{30}$$

From Equation (30), it is evident that the influence of $K_{be}$ on $P_a$ is small and therefore, can be omitted to obtain an initial estimate of $P_a$. When the system is activated, however, the steel members only carry the force $F$ while the tensioning elements accommodate the additional brace elongation through elastic deformations. Therefore, the brace load at a positive tensile deformation, $\delta^+$, is given by:

$$P^+ = F + T_{p0} + K_p \delta^+ \tag{31}$$

Upon unloading, the frictional mechanism locks and the initial brace stiffness, $K_{be}$, is recovered. The behavior of the SCED brace element under compressive deformation is similar to that of the tensile deformation except that the steel members must resist the total compressive axial load and the pretension of the tensioning elements. Also, the axial shortening of the members reduces the axial deformation demand on the tendons ever so slightly, and therefore, the brace force and the axial stiffness are slightly reduced as well (Christopoulous et al., 2008).

Once the relationship between the various design parameters and the overall behavior of the SCED element has been established, the steel members, tensioning elements, and the properties of the friction mechanism can be selected in order to obtain the desired axial brace strength and energy dissipation capacities.

## 2.3 Hybrid Braces

### *2.3.1 Background and Current Practice*

The last type of high-performance brace this thesis will address is the hybrid brace frame. The concept of a hybrid brace frame may refer to the multiple types of devices and the countless number of various configurations within each type that exist in designing lateral resisting systems. More specifically however, the hybrid passive control device (HPCD), as developed by Marshall and Charney (2008), will serve as the focus of this section and will represent the general concept of the hybrid brace frame.

According to Marshall, the HPCD is a combination of two typical passive control devices combined in a new way to create a unique and innovative device, which enhances the strengths and offsets the weaknesses of the individual devices (Marshall, 2008). The HPCD is a two-stage device: the first stage is a viscoelastic solid device consisting of a high damping rubber (HDR) material, and the second stage is a hysteretic yield device much like that of the BRB brace element. The first stage provides energy dissipation for all deformation levels such as wind events and minor to moderate earthquakes without the need for brace yielding, while the second stage, which only engages during severe deformations, provides the ability to dissipate significant energy during major seismic events. The second stage, when activated, also provides additional stiffness to the brace element and in turn to the overall lateral system for reduced floor displacements, helping to mitigate instabilities from forming in the structure. Furthermore, the tiered hysteretic yielding stage of the HPCD allows the system to limit the structural damage at only the aforementioned elements, allowing for less conspicuous repairing of the whole structure.

### *2.3.2 High-Performance Aspects*

Not unlike the SCED brace, the HPCD builds on the basic concept of the BRB with the added benefit of staging the energy dissipation through member yielding only in major lateral deformation levels, and allowing for the viscoelastic damping device to dissipate energy from less significant events. The use of a high-damping rubber (HDR) is not in any way novel and has been widely used in base isolation schemes. Due to their exceptional energy dissipating capacity, the HDR has been adopted by the HPCD concept to act as an elastomeric damping material in braces.

The high-damping rubber, as previously noted, has been available to engineers to use as efficient energy dissipating mechanism for quite some time. The material composition of the HDR is a vulcanized natural rubber compound with added carbon black and other fillers to enhance the engineering properties (Marshall, 2008). The addition of carbon black increases the stiffness of the damper and also the loss factor. The fillers are added to reduce the dependence of the material properties of the damper to temperature, loading, and frequency.

The HPCD brace can take on many different configurations, but all conform to the basic concept of utilizing a two-stage energy dissipation mechanism. One possible configuration of the HPCD, using a cylinder type damper brace, is illustrated in the figure below.

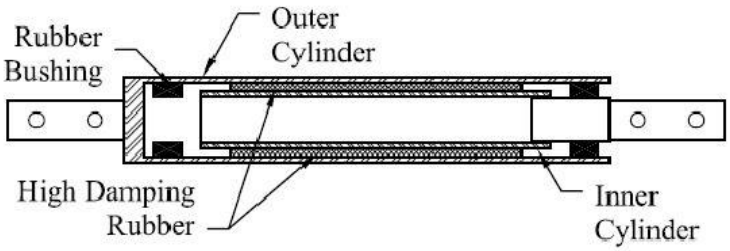


Figure 2.3-1: HPCD Configuration using Cylinder Type Damper (Marshall, 2008)

Another possible configuration of the HPCD is illustrated below, highlighting the use of a metallic yielding device, referred to as a tapered plate energy absorber (TPEA), in parallel with a viscoelastic damper such as the HDR.

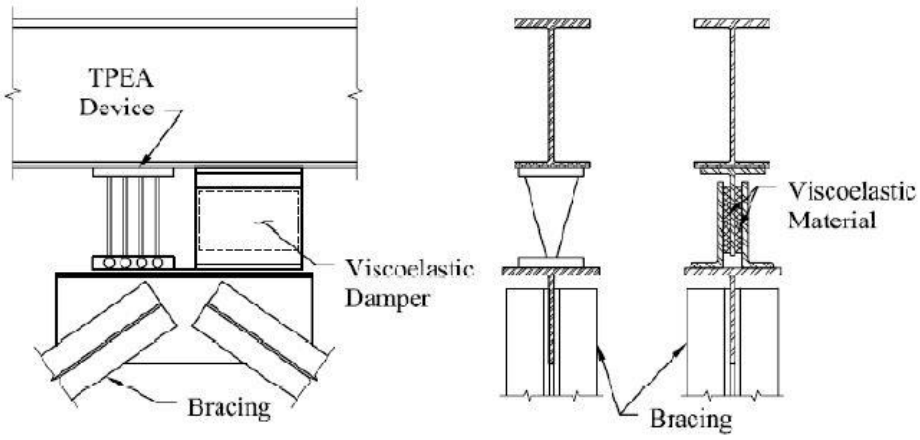


Figure 2.3-2: HPCD Configuration using TPEA and VE HDR in Parallel (Marshall, 2008)

### *2.3.3 Design Methods, Mathematical Formulation, and Modeling Considerations*

To understand the behavior of the HPCD brace, it is critical to correctly formulate and model the behavior of the HDR material. The development of the HPCD by Marshall (2008) outlines a primer for formulating the complex behavior of the rubber material and modeling the element in finite element analysis software. The complexity arises from the fact that rubbers can be classified as both an isotropic and a viscoelastic solid. The HDR material has two aspects to its behavior: the first being the time-independent force-deformation response, the other being the time dependent loss modulus. Although the behavior of the HDR damper depends heavily on the subtle material composition as well as the complex dual nature of the loss modulus, the general hysteretic behavior can be obtained for the HDR, as shown below.

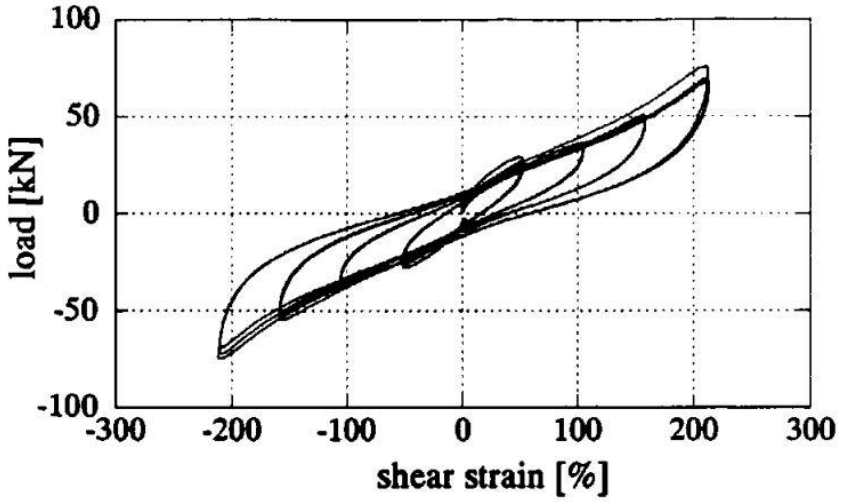


Figure 2.3-3: HDR Force-Deformation Relationship (Abe et al., 2004)

# Chapter 3

# Model Definition

The purpose of this chapter is to describe the formulation of the analysis model created in SAP2000 to evaluate and compare the structural performance of the three high-performance brace types. A brief description of the building and its site location will be presented, followed by an overview of the pertinent building codes, then the modeling considerations for the various types of brace elements.

## 3.1 Building Description

A well-defined, fully code-compliant, prototype building was developed as a basis for comparison of the three high-performance braces presented in this thesis. The building is a six-story steel structure, which is representative of a very common building type in an area of high seismicity. The building profile embodies a rectangular plan spanning 150'-0" in the

X-Direction and 180'-0" in the Y-Direction, with columns spaced at 30'-0" on center. The height of the building is 72'-0" above ground with two subgrade levels totaling 24'-0" in depth, with typical floor to floor heights of 12'-0". The subgrade structure is comprised of 14" concrete retaining walls along the perimeter of the building at the lower basement level and 10" walls at the upper basement level. Each floor diaphragm of the superstructure consists of a 3½" lightweight concrete slab on a 3" metal deck. Lastly, the building is enveloped by a glass curtain wall façade along the entire perimeter of the structure up to the roof. A three-dimensional perspective of the building is shown below, followed by the plan and elevation views from each of the two principal directions.

The brace layout can be visualized in the plan view of the building, Figure 3.1-2, with two braced bays per principal direction. All of the braces in the base model are a concentrically braced frame configuration, also known as a chevron brace, as shown in the elevation views. This configuration is used as a control in comparing the three different types of high-performance braces to isolate the changes in performance of the structure to the type of brace rather than the configuration.

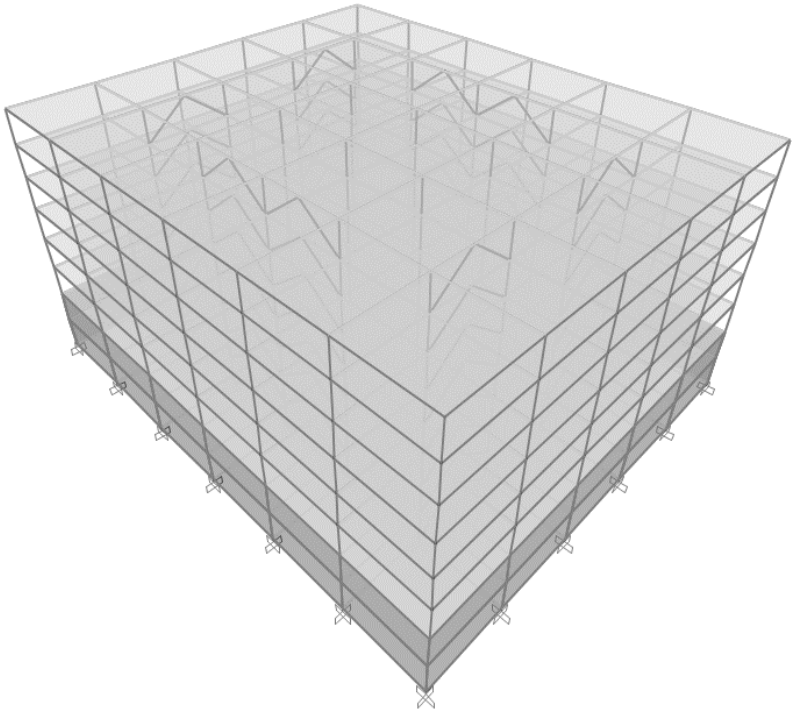

Figure 3.1-1: Isometric Perspective View of Base Model

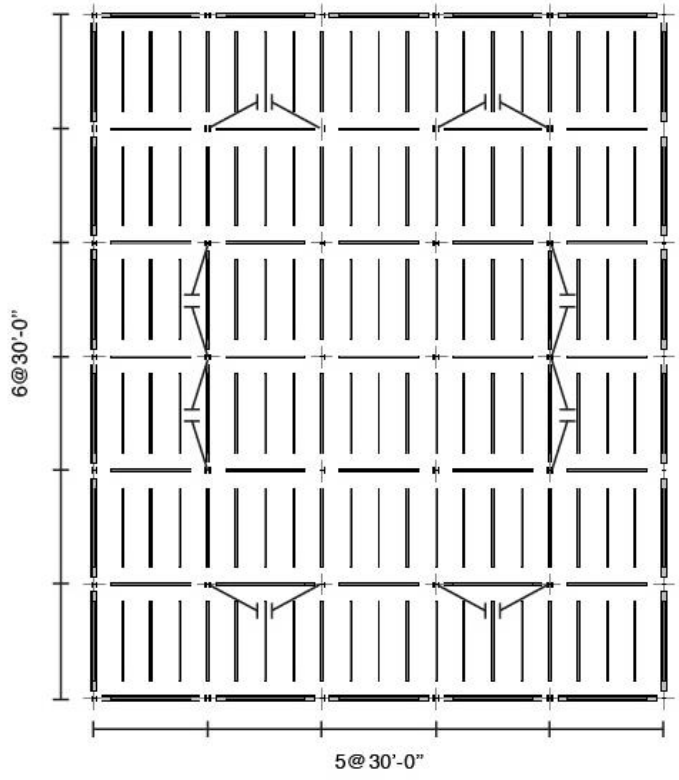


Figure 3.1-2: Plan View of Base Model

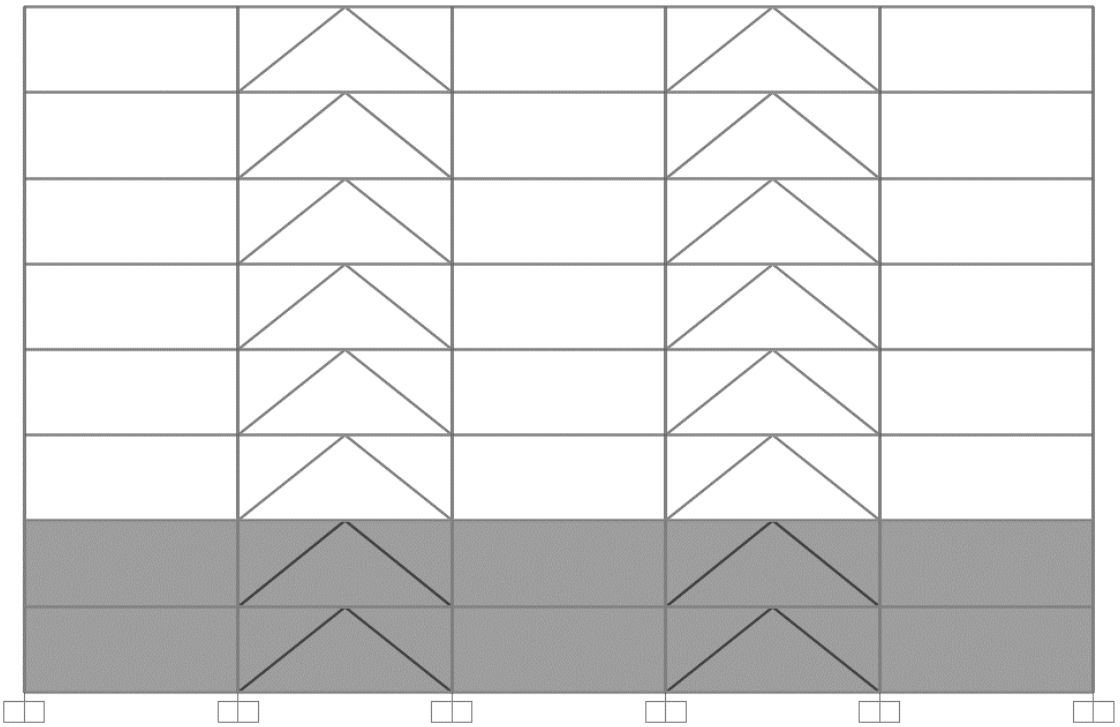

Figure 3.1-3: Elevation View of Base Model in the X-Direction

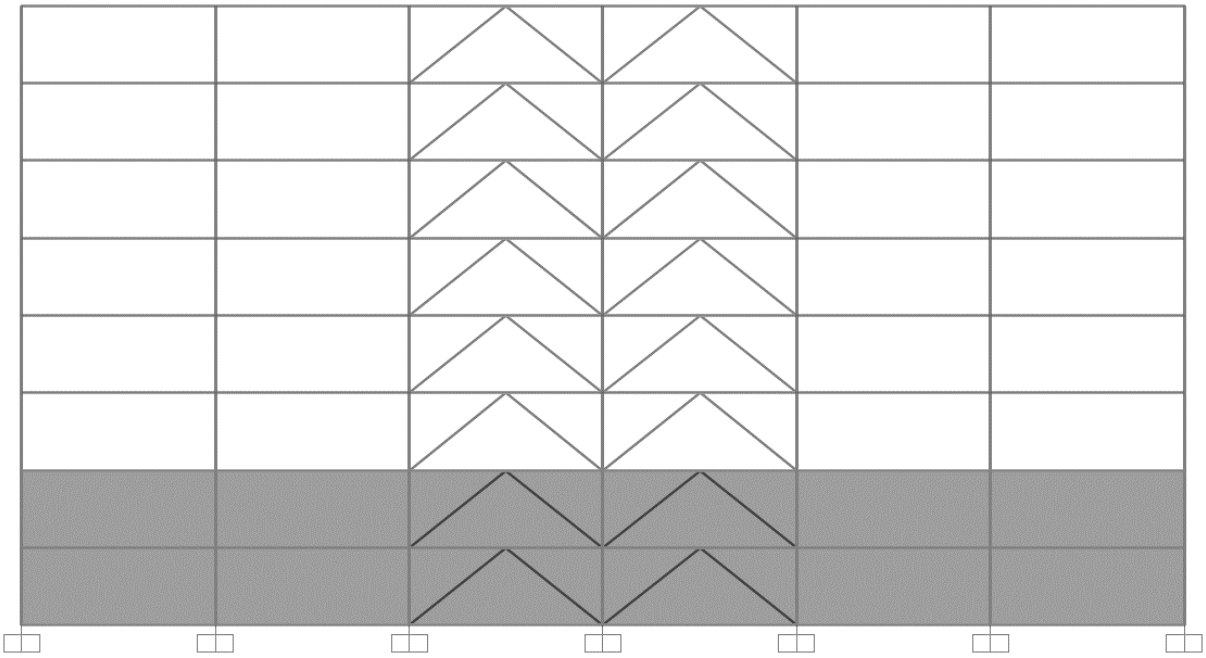

Figure 3.1-4: Elevation View of Base Model in the Y-Direction

## 3.2 Code-Based Design of Base Model

The prototype building was designed to be used as an office building in downtown Berkeley, CA, which is an area of high seismicity where the benefits of high-performance braces can be best realized. The site location dictated the seismic demands as well as the soil profile for the building in designing adequate lateral systems. Tabulated below is the seismicity information for the respective site location of the building. Furthermore, the prototype building adheres to the typical design considerations for office buildings with regards to occupancy category and importance factor as per ASCE 7-10.

| Period | $S_a$ (g) | $S_{DS}$ (g) | $S_{D1}$ (g) |
|---|---|---|---|
| T = 0.2s | 3.0467 | 2.0311 | - |
| T = 1.0s | 1.1705 | - | 0.7804 |

Table 3.2-1: Site Seismicity Parameters (USGS Earthquake Hazards Program)

The structure also incorporates subgrade levels to most realistically model the column boundary conditions at ground level, since many office buildings typically include basements (Fahnestock, 2006). The gravity system was designed in accordance to the codes ASCE 7-10 and AISC Steel Construction Manual. The frame elements are all wide-flange steel sections, and the beams and girders take advantage of composite action with the floor slabs.

The lateral system of the building is comprised of the concentric braces in the corresponding bays as described in the previous section, supplemented by the moment framing of the columns and girders throughout the rest of the structure. The initial design of the braces was obtained from the equivalent lateral force method as per the International Building Code (2009), and sized for an earthquake with a 2% probability of exceedence in 50 years, and a mean return period of approximately 2,500 years. The ground acceleration values pertaining to the design earthquake are tabulated in Table 3.2-1. Finally, the prototype building was designed to achieve a Life Safety Building Performance Level for the 2,500-year earthquake as per the ASCE 41-06 Seismic Rehabilitation of Existing Buildings code.

## 3.3 Modeling High-Performance Braces

The prototype building, as outlined in the previous section, was developed in order to create a control or a base model for the comparative study of the high-performance braces. The lateral system in the base model was initially designed using the equivalent lateral force method to meet code requirements for both strength and displacement including second-order effects. This code-compliant base model was then altered to create a modified frame for each of the three types of high-performance braces: the BRBF, SCED, and HPCD. A special moment resisting frame (SMRF) was also developed off the base model, by removing the concentric braces and stiffening up the frame with heavier beams and columns to meet the same code criteria, to serve as yet another subject for comparison.

In modeling the BRBF elements, the design procedure as more thoroughly outlined in the literature review section was considered to accurately account for the increase in stiffness of the BRB. The cross-sectional area of the BRB steel core was modeled as approximately 40% greater than that of the actual core area of brace obtained in the design, to account for the following factors: the partial fixity inherent in the brace end connections, the additional stiffness from the increase of cross-sectional area of the non-yielding portion of the steel core at each end of the brace element, and the small increase in stiffness from the encasement material as well as the steel tube that confines the brace element (Seamer, 2007).

The nonlinearity of the structure as well as that of the high-performance braces was accounted for in the model through the use of discrete non-linear hinge elements. The beams and girders are all assigned with flexural hinge elements including strain hardening about the strong axis at a distance of 10% from the members' end. The columns were not expected to yield but were also modeled with an interacting axial load-bending moment plastic hinge at each end.

The BRB elements were modeled as non-prismatic sections divided into three segments. The middle 75% of the brace's length was modeled as the yielding steel core, with the appropriate cross-sectional area as determined and described in the previous paragraph, while the two ends, each 12.5% of the member's length, were modeled using a rigid offset from the end connections. The discretization of the BRB element allows for a more accurate representation of the brace formulation that accounts for both the yielding steel core and the non-yielding

brace end connections. Since nonlinearity was restricted to only the middle portion of the BRB element, the braces were assigned with nonlinear axial hinge elements at the midpoint of the central segment (Seamer, 2007). The properties pertaining to the nonlinear hinge elements were designed to adhere to the guidelines provided by the FEMA provisions for seismic design (FEMA 356, 2000). Illustrated below is a generalized moment-rotation and axial load-deformation relationship for hinge elements as per FEMA guidelines.

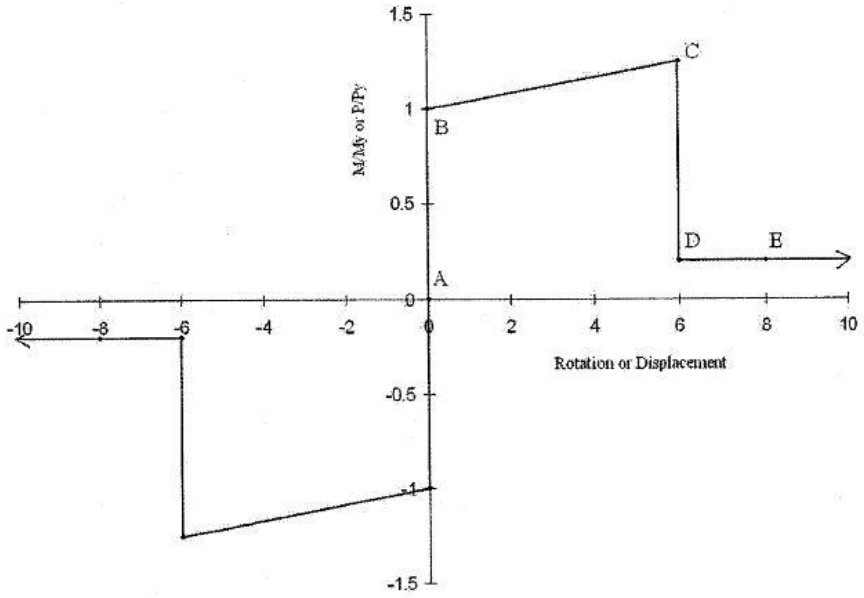


Figure 3.3-1: Generalized Moment-Rotation and Axial Load-Deformation Relationship for Hinge Elements (Seamer, 2007)

The energy dissipation elements found in SCED and HPCD braces were modeled using a combination of linear and nonlinear link elements in tandem with the modeling considerations of the BRB element. The tensioning element of the SCED brace is modeled with a multilinear plastic spring in parallel with the BRB brace, representing the two-stage behavior of the shape memory alloy wires. The high-damping rubber damper device in the HPCD brace is modeled using a multilinear elastic spring in parallel with a linear viscous damper dashpot. The multilinear elastic spring element provides the ability to model the behavior of several legs of different elastic stiffness, necessary in representing the initial stiffness of the HDRD followed by an increased stiffness when the locking mechanism engages (Marshall, 2008). The figures below illustrate the configuration of the link elements modeled for the HPCD brace, as well the type of spring used to represent each link.

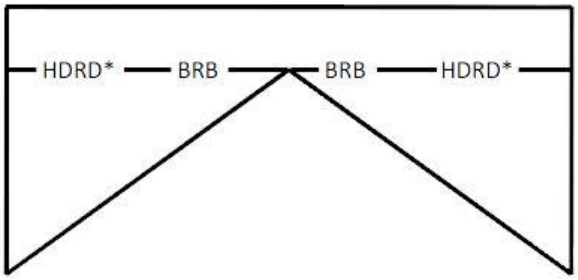


Figure 3.3-2: Diagram of HPCD Hybrid Energy Dissipation System (Marshall, 2008)

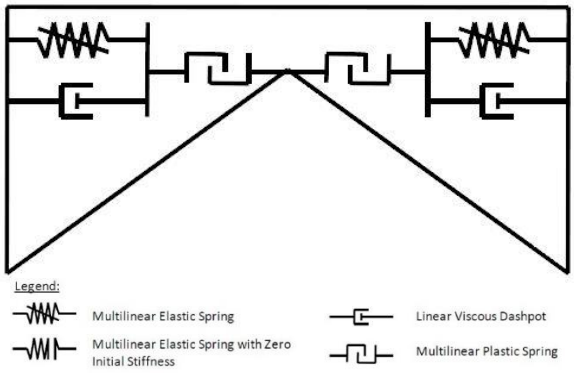


Figure 3.3-3: Modeling of HPCD Hybrid Energy Dissipation Configurations (Marshall, 2008)

Lastly, Rayleigh proportional damping of 2% in the first and fifth modes was included for each of the high-performance brace models. However, Rayleigh damping only represented the inherent damping of the structure; the additional damping provided by the hysteretic behavior of the various brace elements was different for each model. The HPCD brace element in particular, which includes the HDR damper device, required an iterative process involving the log decrement method to achieve the appropriate damping constant of the dampers to achieve a total model damping of approximately 10% (Marshall, 2008).

# Chapter 4

# Analysis Procedures

As stated in the *Introduction,* one of the primary aims of this thesis is to compare and evaluate the various types of high-performance brace systems with regards to its structural performance benefits. This chapter will present an overview of the analysis procedures pertinent to seismic design and also provide the methodology used to analyze the high-performance brace models to convey the proposed results.

## 4.1 Overview

Four modified analysis models, each built on the base model described in the previous chapter, were generated for analysis: the buckling-restrained brace frame, self-centering energy dissipating brace frame, hybrid brace frame, and lastly, the special moment resisting frame. Each high-performance brace frame was then analyzed using a nonlinear response history

analysis method as will be described in the sections to follow. There are six commonly recognized structural analysis methods allowed by code to use in designing earthquake-resistant structures (SEAOC Seismology Committee, 2009). Each analysis procedure can be classified according to whether a linear or nonlinear model of the structure is subjected to a static or dynamic analysis. Tabulated below summarizes the aforementioned analysis procedures with the corresponding model properties and type of analysis.

| | | **Structural Model** | |
|---|---|---|---|
| | | **Linear** | **Nonlinear** |
| **Analysis Method** | **Static** | (1) Simplified Analysis<br>(2) Equivalent Lateral Force Analysis | (3) Nonlinear Static Pushover Analysis |
| | **Dynamic** | (4) Modal Response Spectrum Analysis<br>(5) Linear Response History Analysis | (6) Nonlinear Time History Analysis |

Table 4.1-1: Seismic Analysis Procedures (Adapted from SEAOC Seismology Committee, 2009)

The selection of which seismic analysis procedure can be chosen depends on a combination of various design parameters such as: the seismic design category, seismic use group, structural material, and structural configuration, which includes building characteristics such the height, period and irregularity. The following paragraphs will describe each analysis procedure in detail to rationalize the particular procedure chosen to analyze the high-performance brace frames. From this point onwards, the analysis procedures will be termed (LSP) for the linear static procedure, (LDP) linear dynamic procedure, (NSP) nonlinear static procedure, and lastly, (NDP) for the nonlinear dynamic procedure.

## 4.2 Linear Static Procedure

The Simplified analysis, according to the SEAOC Seismology Committee, is a conservative version of the more general equivalent lateral force analysis, and thus, does not require a drift check. The ASCE 7-10 allows the Simplified analysis for buildings not exceeding three stories in height, in Occupancy Categories I and II, and in Site Classes A-D. This LSP method is generally intended for use in relatively simple buildings, hence is not chosen for the analysis of the high-performance brace models.

The second type of LSP, the Equivalent Lateral Force method (ELF), is the most commonly used seismic design procedure, and has been codified in various forms for several decades (SEAOC, 2009). The ELF method determines the design seismic forces from a linear elastic static analysis of the structure, and in effect, removes the time-varying inertial forces due to earthquakes by an equivalent set of static forces applied to each floor of the building. This method also implicitly assumes that all mass participates in the first mode of the structure. To counter this assumption, the distribution of the lateral force can be altered to address the contributions of higher modes, but research shows that even then, base shears determined in more accurate nonlinear analyses can significantly exceed the values obtained from the ELF method (Eberhard and Sozen, 1993). Furthermore, the ELF method is recognized to be inadequate for structure with: irregular distributions of mass and stiffness, non-uniform story strengths, strong coupling of the translational and torsional responses, and flexible diaphragms on multiple floor levels (SEAOC, 2009).

The ELF method, due to its inherent elastic nature, cannot accurately capture the force and deformation demands of the structure under inelastic response. Therefore, for structures with a seismic design modification factor $R$ greater than 1.5, nonlinear analysis procedures may be better suited to accurately model seismic behavior. However, the ELF method is often used as a benchmark for scaling of the base shears and other response quantities obtained from dynamic analyses, and therefore, was utilized to initially design the base model as described in Chapter 3. Codes generally allow for the preliminary design of lateral force resisting systems to use the ELF method in determining the required base shear strengths to be later supplemented by further dynamic analyses for performance quantities that are strongly sensitive to influence from higher modes such as story shears and interstory drifts (SEAOC, 2009).

## 4.3 Nonlinear Static Procedure

The NSP includes a variety of analysis methods that are all based on static pushover analyses of a nonlinear model, including procedures such as the Capacity Spectrum Method, Displacement Coefficient Method, and the various adaptive and multiple mode pushover techniques. In all variations of the NSP, a nonlinear model of the structure is subjected to gradually increasing lateral forces and the overall behavior of the structure is observed. Since the nonlinear behavior of the structural elements is modeled, the structure displays inelastic

behavior once yield point is exceeded. The global behavior can be characterized by a capacity curve, plotting the base shear as a function of displacement of a control point, to illustrate the inelastic effect.

The static pushover analysis can be useful in estimating deformation demands and determining the required strength and stiffness, as well as the ductility demands of the lateral system. However, the NSP, as with the LSP, has significant limitations in that the analysis does not represent the contributions of higher modes. Although the higher modes typically contribute very little to displacement demands, their contribution to interstory drifts and story shears is not negligible, and thus the NSP is inadequate for analysis of high-performance brace frames where performance criterion such as interstory drifts is of critical importance (SEAOC, 2009).

## 4.4 Linear Dynamic Procedure

The LDP analysis comprises of two main methods, the Modal Response Spectrum Analysis and the Linear Response History Analysis. Both LDP analysis methods inherently account for the contribution from higher modes, but still use a linear elastic model in conjunction with scaling to the ELF base shear to determine design forces. The main difference between the LSP and LDP methods is the distribution of lateral forces over the building height to more accurately account for the effects of irregularities due to the higher modes. However, the design forces obtained from the LDP can be drastically inaccurate for structures in which significant nonlinearity is expected. Therefore, the high-performance brace frames, which intrinsically embody nonlinear behavior by precluding the yielding of some structural elements, may not be best suited for analysis using the LDP methods.

In the Modal Response Spectrum Analysis, according to the SEAOC Seismology Committee, the peak modal responses are combined using modal combination rules such as the SRSS or CQC rules as an approximation to the actual time-varying interaction of the modes. The orthogonality of the undamped modes of vibration allows the linear elastic response to be represented by superposing the responses of the individual modes in time. The number of modes to be accounted for is determined by the requirement of at least 90% of the participating mass to be represented in the analysis. It is important to note that code-specified elastic design spectra that are typically used in the Modal Response Spectrum

Analysis has inherently unrealistic representation of demands due to imperfections in calculating the probabilistic spectral ground motions, which are different for every seismic event and source. Therefore, the uniform hazard design spectrum is generally an overestimation of the contribution of all modes at the specified design earthquake exceedance probability (SEAOC, 2009).

The Linear Response History Analysis determines the response history of the structure from a step-by-step solution in the time or frequency domain to a signal that represents the motion of the ground. The calculation method can involve the use of modal superposition as outlined above, with the sufficient number of modes to represent at least 90% of the participating mass, or by direct integration, which inherently represents the entirety of the mass associated with the structure. The responses computed using this method are for a particular ground motion record, and therefore, are a function of only the specific excitations that have been used in the calculation. A set of linear response history analyses can then be performed for a more exhaustive understanding of the response of the structure, which can also be appended to other procedures to gauge the effects of the higher modes. However, as mentioned earlier in this section, both LDP methods intrinsically use the linear elastic model in determining the response of the structure, and therefore, are inadequate for the analysis of high-performance brace frames.

## 4.5 Nonlinear Dynamic Procedure

The last type of seismic analysis, and fittingly the most complex, is the nonlinear dynamic procedure. The NDP essentially embodies the same analysis methods as the LDP, but accounts for nonlinearities by using a nonlinear inelastic model in the analysis. This method is considered to be the most accurate of the analysis procedures because it closely represents the inelastic response of the structure, and has become the benchmark by which the accuracy of other procedures is evaluated (SEAOC, 2009). The NDP inherently accounts for the contribution of higher modes and the influence of nonlinear component behavior on the response of the structure, and thus, is most suitable for the analysis of high-performance braces. It is critical to note that in nonlinear response history analysis, the nonlinearity causes coupling between the modes, and therefore the peak response from each of the modes cannot simply be superposed, but rather all modes must be analyzed simultaneously in order to perform modal combination at each time step (Wong, 2011).

The nonlinear response history analysis method using direct integration was ultimately chosen to analyze the high-performance brace frames. The complexities of the nonlinear hinge definitions as well as the multilinear elastic and plastic link components of the high-performance braces, as outlined in Section 3.3, necessitated the exhaustive analysis method. Although the direct integration method is computationally less efficient than a modal response history analysis, it allows the behavior of the nonlinear hinge elements to be directly considered at each time step during the analysis (Seamer, 2007).

Each of the high-performance brace models was subjected to a suite of seven scaled ground motion records that represent a wide range of different historical seismic events. A table summarizing the ground motion records used in the analysis is tabulated below, and the acceleration plots for each of the records can also be found in Appendix A.

| Earthquake | Year | Station | Magnitude | Distance (km) | PGA (g) | PGV (cm/sec) | PGD (cm) |
|---|---|---|---|---|---|---|---|
| Imperial Valley | 1979 | El Centro | 6.53 | 28.09 | 0.5379 | 56.8 | 32.99 |
| Superstition Hills | 1987 | Brawley | 6.54 | 29.91 | 0.1349 | 15.9 | 7.04 |
| Victoria, Mexico | 1980 | Chihuahua | 6.33 | 36.67 | 0.1179 | 19.73 | 9.97 |
| Duzce, Turkey | 1999 | Duzce | 7.14 | 1.61 | 0.4273 | 70.77 | 47.3 |
| Chalfant | 1986 | Bishop | 6.19 | 20.27 | 0.2058 | 19.32 | 6.97 |
| Northridge | 1994 | Rinaldi | 6.69 | 10.91 | 0.6336 | 109.24 | 28.26 |
| Erzican | 1992 | Erzican | 6.69 | 8.97 | 0.4886 | 72.95 | 24.79 |

Table 4.5-1: Summary of Ground Motion Records Used in Time History Analysis (PEER NGA)

Each earthquake used in the analysis included the four components of the seismic record: the fault normal (FN), fault parallel (FP), geometric mean (GM), and the vertical (Vert). Only the geometric mean of the FN and FP components is reported in the summary table above, but the time history analysis was conducted with all twenty-eight components of the set of seven earthquakes. The graph below shows the entire set of the scaled response histories used in the analysis, followed by the geometric and arithmetic mean spectra overlaid on the target design spectrum. The direct integration time history analysis used the Hilber-Hughes-Taylor (HHT) method with a time step size of 0.01 seconds (Hughes, 1987). Although a nonzero alpha value in the HHT method can be useful to damp out the response from very low periods, using the value of alpha equal to zero is most accurate (CSI, 2013).

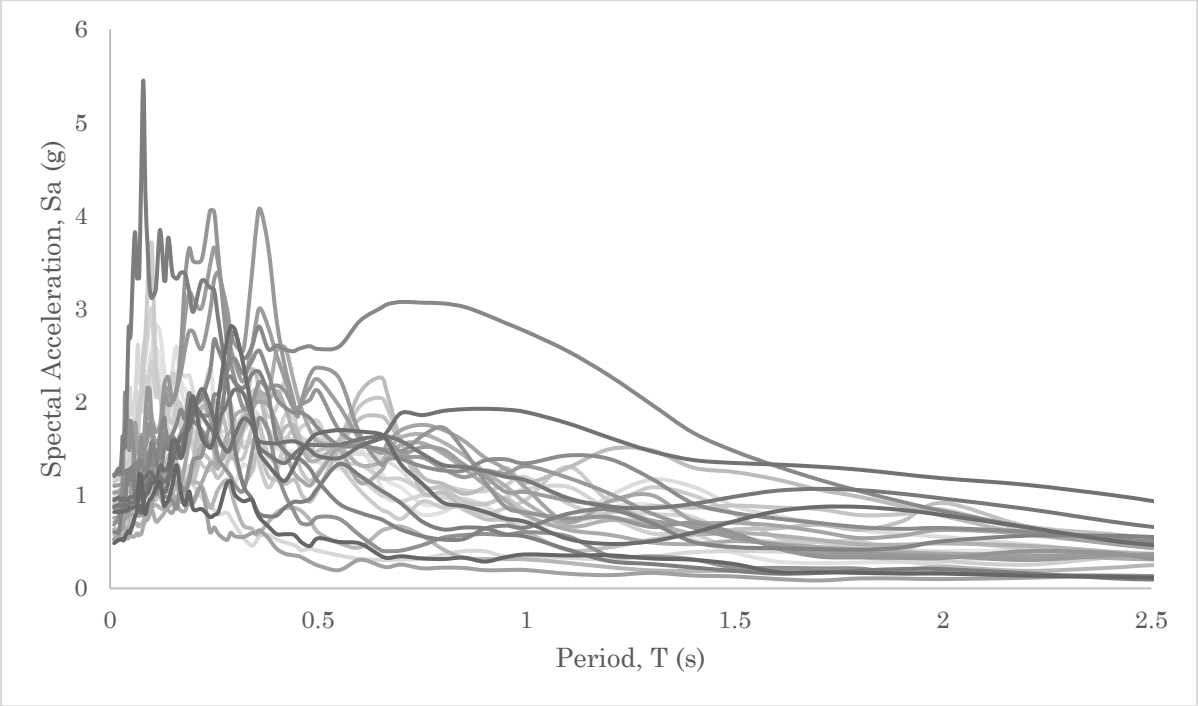


Figure 4.5-1: Scaled Response Histories of All Four Components of Ground Motion Records

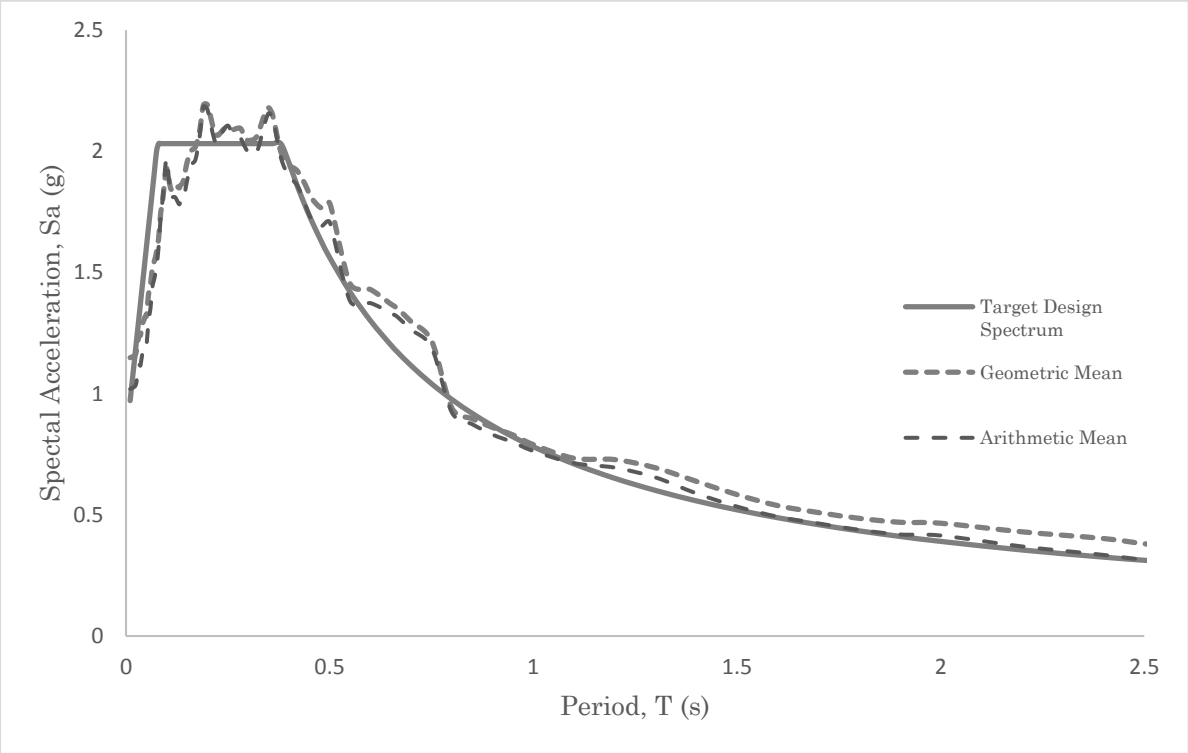


Figure 4.5-2: Target Design Spectrum with Scaled Geometric & Arithmetic Mean Spectra of Ground Motion Records

# Chapter 5

# Analysis Results

The structural analysis program SAP2000 was used to perform the nonlinear response history analyses on the high-performance brace models. This chapter will present the following results in order: peak floor displacements, peak interstory drift ratios, peak interstory residual drift ratios, and peak floor accelerations. These performance parameters will then be discussed to illustrate the various benefits and possible shortcomings of each of the high-performance braces as compared to each other and to the conventional moment resisting frame.

## 5.1 Peak Floor Displacements

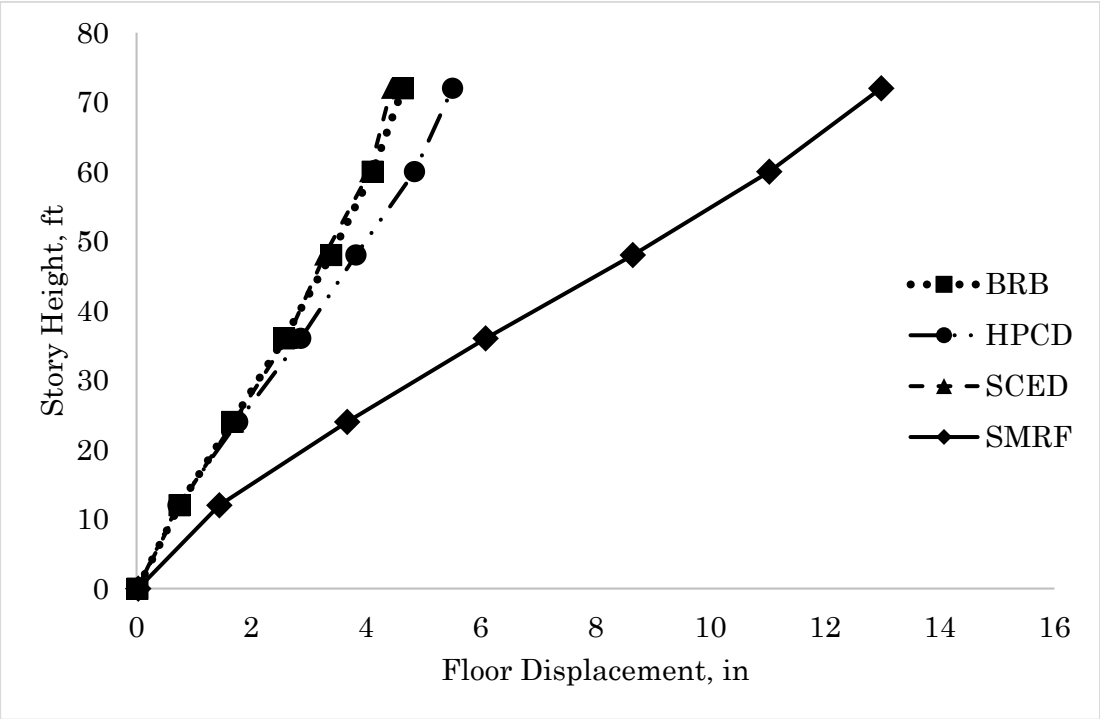


Figure 5.1-1: Peak Floor Displacements as a function of Story Height in the X-Direction

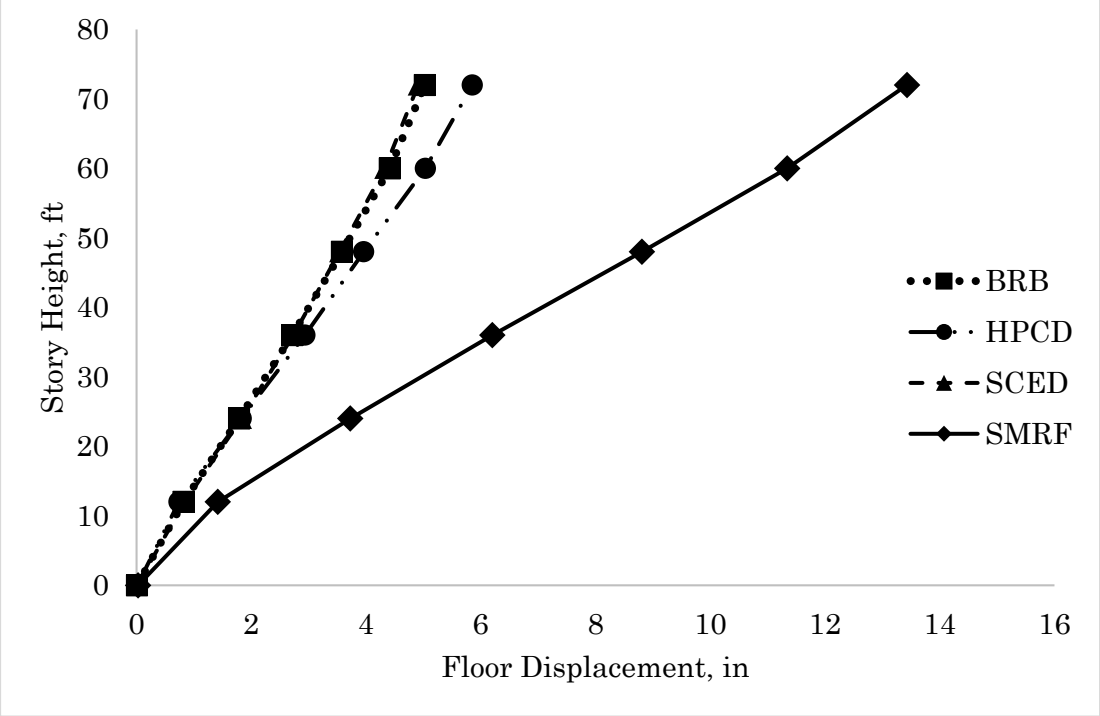


Figure 5.1-2: Peak Floor Displacements as a function of Story Height in the Y-Direction

## 5.2 Peak Interstory Drift Ratios

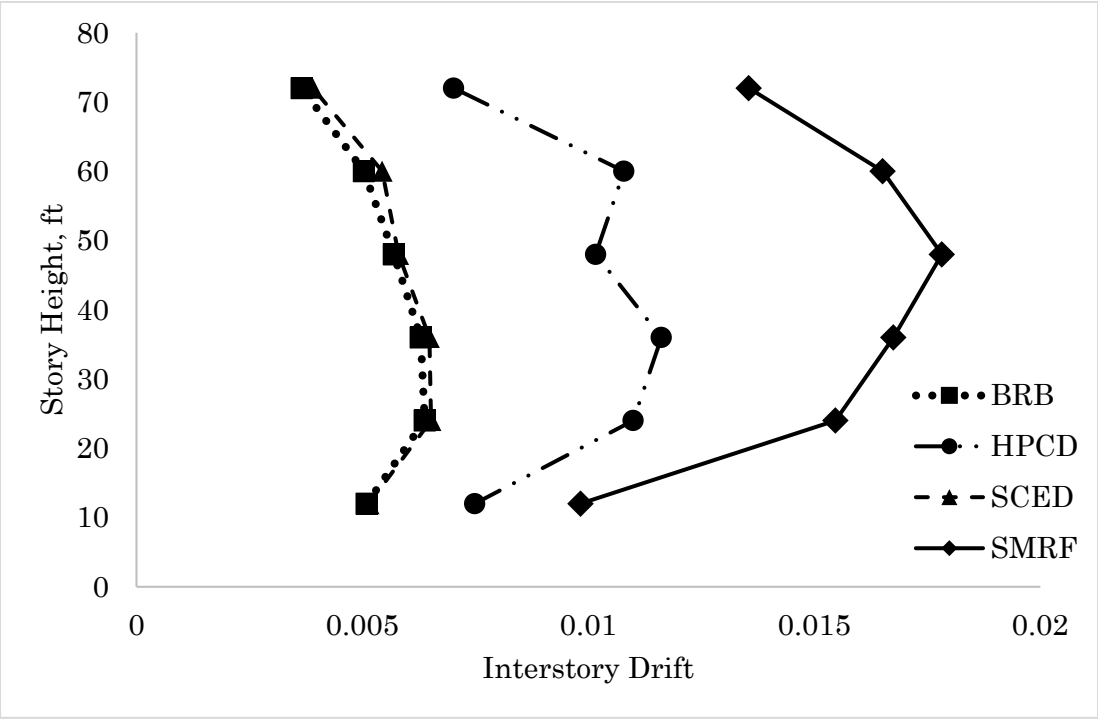


Figure 5.2-1: Peak Interstory Drift Ratios as a function of Story Height in the X-Direction

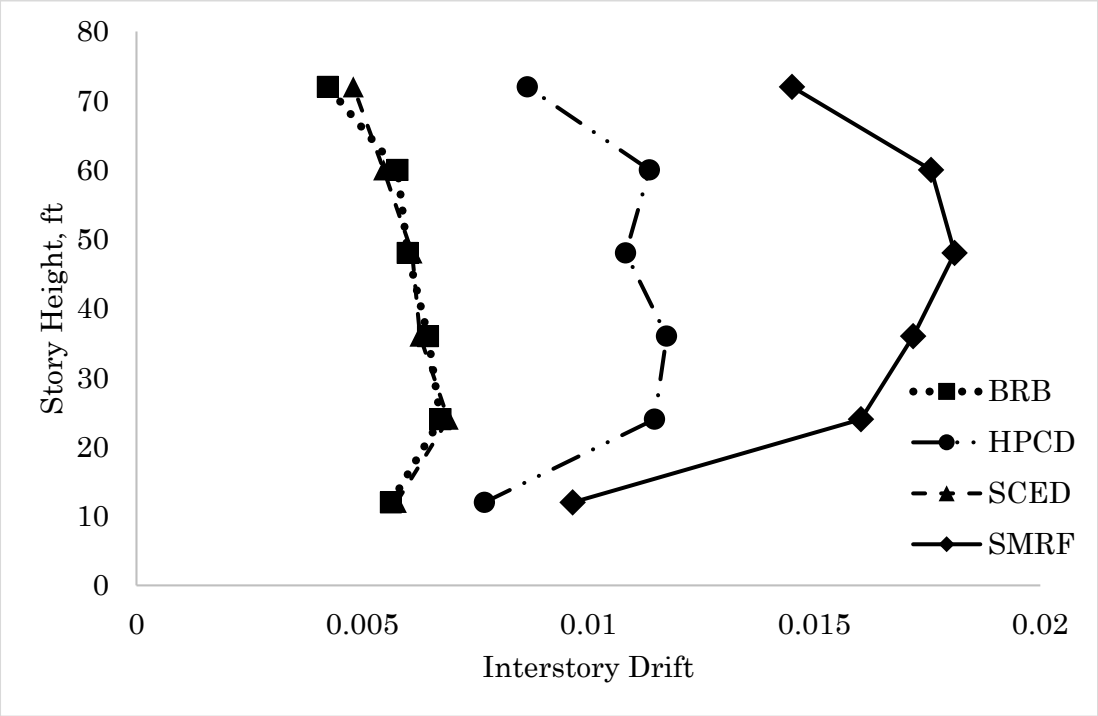


Figure 5.2-2: Peak Interstory Drift Ratios as a function of Story Height in the Y-Direction

## 5.3 Peak Interstory Residual Drift Ratios

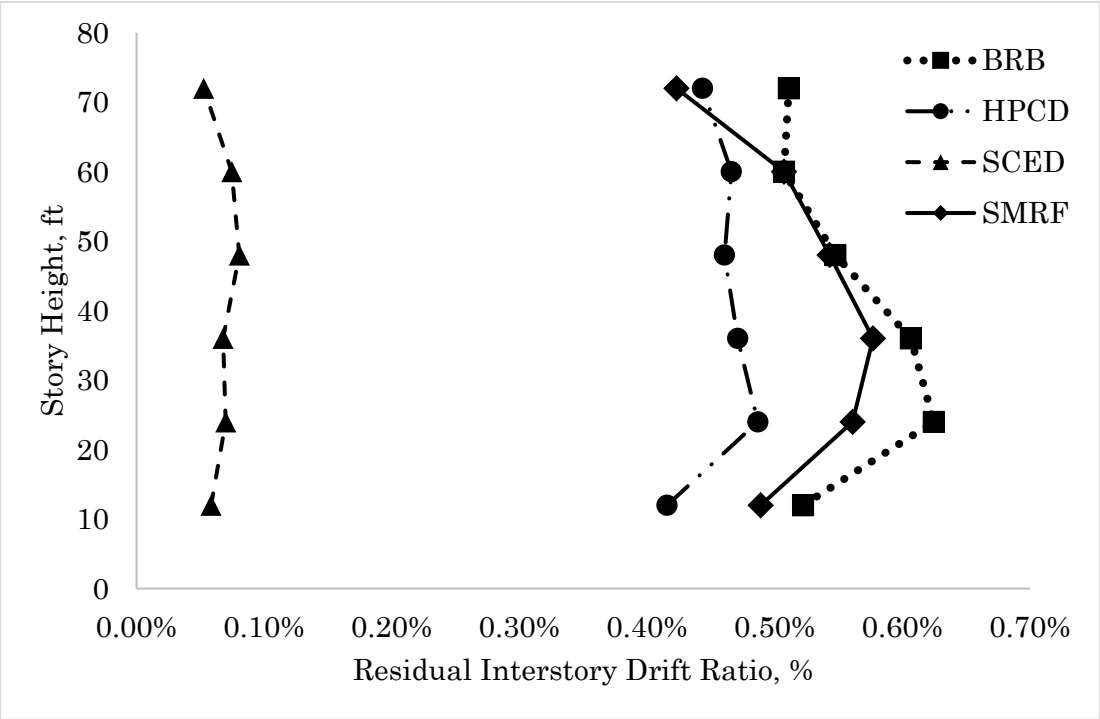


Figure 5.3-1: Peak Interstory Residual Drift Ratios as a function of Story Height in the X-Direction

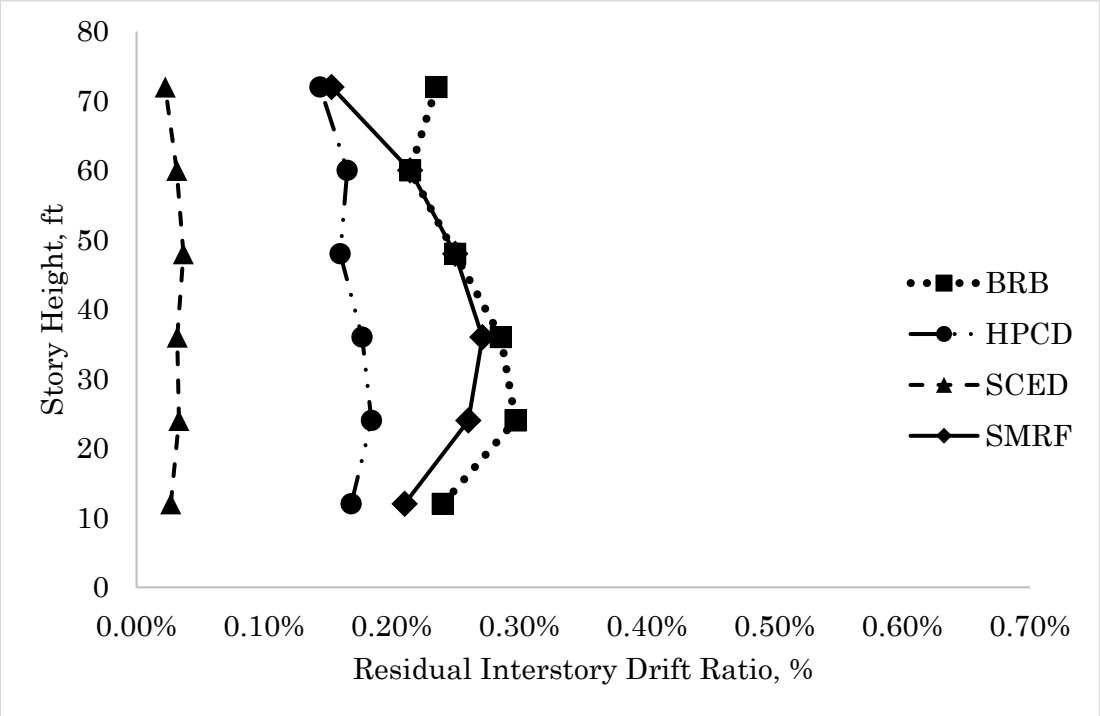


Figure 5.3-2: Peak Interstory Residual Drift Ratios as a function of Story Height in the Y-Direction

## 5.4 Peak Floor Accelerations

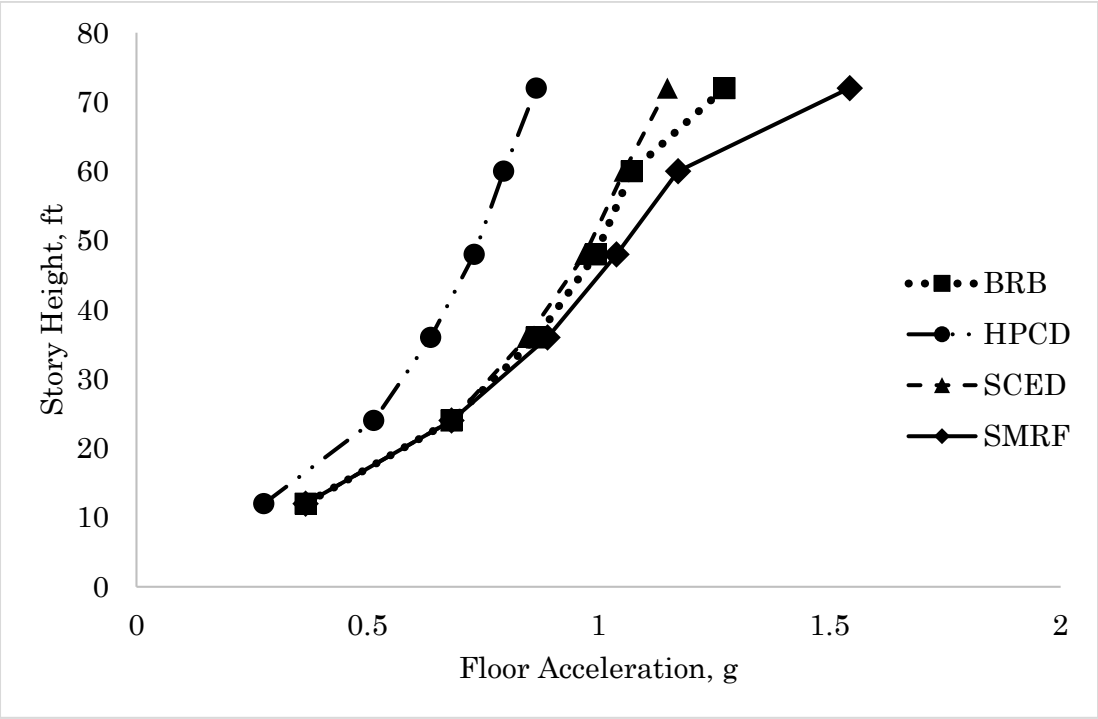


Figure 5.4-1: Peak Floor Accelerations as a function of Story Height in the X-Direction

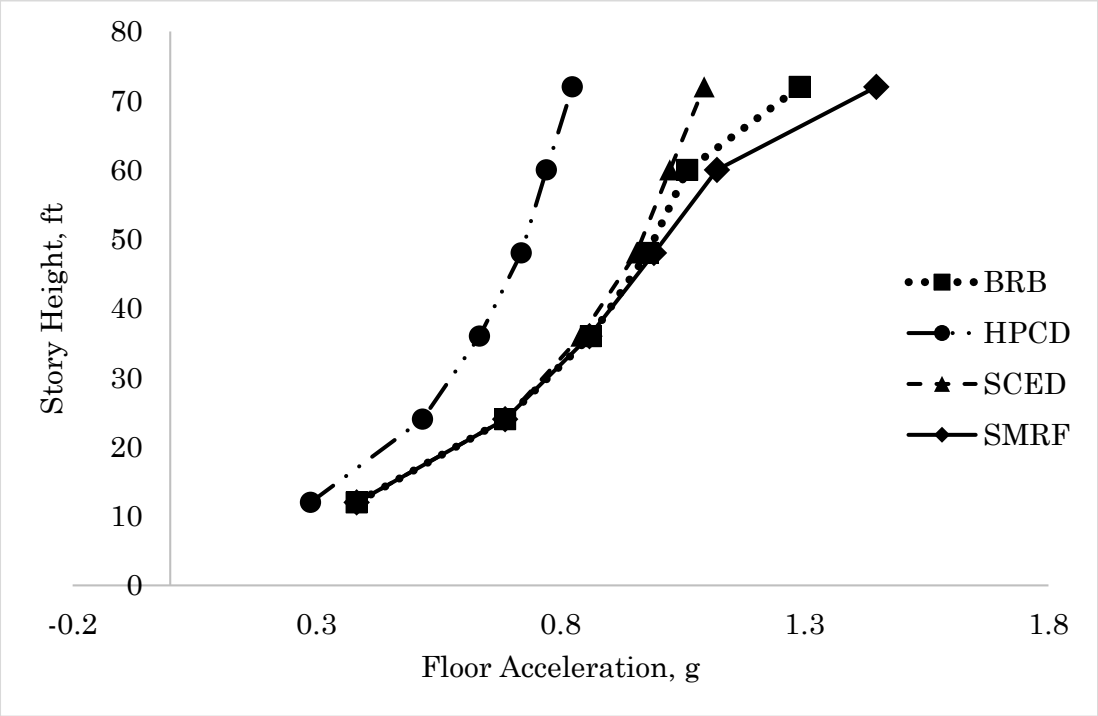


Figure 5.4-2: Peak Floor Accelerations as a function of Story Height in the Y-Direction

## 5.5 Discussion of Results

The four performance parameters presented above, the peak floor displacements, peak interstory drift ratios, peak interstory residual drift ratios, and the peak floor accelerations, are all average quantities of the response of the models subjected to the set of seven ground motion histories.

The first two parameters, the floor displacements and the interstory drift ratios, are primary parameters used to assess the acceptability of a structure in seismic design. These two parameters are presented for both the X-Direction and the Y-Direction of the building. Interstory drift ratios are a measure of how much one story of the building displaces laterally relative to the story below it. Codes pertinent to seismic design require certain interstory drift limits, which are proportional to the Building Performance Level, as per FEMA, chosen for the design of the building.

One of the reasons building codes place limits on interstory drifts is that this performance parameter is directly related to the level of structural damage the building experiences in a seismic event. The initial design provisions for the base model as well as the various high-performance brace models were described more thoroughly in Chapter 3. As evident in the figures illustrating the interstory drift ratio parameter, even the base model, a SMRF, was designed so that the code limit of 2.0% for a Life Safety Performance Level was met.

With regards to floor displacements and interstory drifts, the BRBF and SCED performed significantly better than the SMRF. The interstory drifts for both the BRBF and SCED were in the range of 0.4% to 0.7%. The HPCD resulted in slightly worse drift responses than the BRBF or the SCED, but still performed better than the SMRF. The performance benefits for floor displacements and interstory drifts were expected for the high-performance braces, due to the increased stiffness of the structure provided by the braces, and are confirmed by the results.

The residual drift is another important performance parameter used to assess the soundness of a structure against seismic events. Residual drifts represent the state of the structure at the end of a seismic event, and can serve as a direct measure of the amount of inelastic deformation the structural system experienced during an earthquake. Residual drifts less

than 0.5% are generally considered to be insignificant since this is in the range of acceptable out-of-plumb tolerance for new construction, which is around 0.2% (Choi et al., 2008). For residual drifts between 0.5% and 1.0%, a special assessment by a structural engineer is recommended before the building is reoccupied, and lastly, for drifts greater than 1.0%, some form of seismic retrofitting is required for the continued stability of the structure (Choi et al., 2008).

The results for residual drift show that only the SCED does not require some form of occupancy disturbance. The SCED achieves residual drift ratios less than 0.1% for both directions of excitation. The exceptional self-centering behavior of the SCED brace allows for this particular system to achieve such significantly greater performance levels with regards to residual drifts, as compared to the other high-performance braces. The relatively high levels of residual drift found in the BRBF, HPCD, and the SMRF are mainly due to the fact that the entire displacement of the system results in an unrecoverable deformation until the system is loaded in the opposite direction (Choi et al, 2008).

Lastly, with regards to the peak floor accelerations, the BRBF and the SCED do not provide any noticeable performance advantages over the SMRF. While the increased stiffness of the BRBF and the SCED provided significant benefits in floor displacements and interstory drifts, it proportionally increased the floor acceleration response as well. However, as illustrated in the floor acceleration graphs above, the response of the BRBF and SCED are comparable to that of the SMRF, which is a good indication that the BRBF and SCED provide adequate ductility as well as sufficient stiffness. The HPCD, on the other hand, performed best in this category, yielding the lowest floor accelerations throughout the entire height of the building. The decrease in acceleration response is mainly achieved through the additional damping of the HPCD, which is embodied in the inherent damping of the HDR damper device.

# Chapter 6

# Economic Feasibility

The purpose of the following chapter is to provide introductory insights into the economic aspects of implementing high-performance braces. The benefits in structural performance alone are not enough to convince engineers to adopt the use of these new systems. Therefore, the economic feasibility of the various high-performance braces is presented to better outline the overall consequences of adopting such systems. This chapter will discuss the possible economic benefits in implementing high-performance braces by presenting several case studies and their implications.

## 6.1 Buckling-Restrained Brace Frames

It may seem that due to the rather contemporary nature of the development of high-performance braces, economic feasibility would be the primary challenge for their practical implementation. However, there is sufficient evidence to show that it is quite the contrary. Studies commissioned by StarSeismic™, one of the most widely known BRB manufacturers in the USA, have shown clear evidence in supporting this claim.

Dasse Design Inc. (2009), conducted an analytical study to investigate potential material savings and cost advantages of utilizing a BRBF system as opposed to the conventional CBF system. Model buildings of two different heights, a three-story structure and a six-story structure, were developed for each of the two lateral force resisting systems. Both models were designed as per code with typical building characteristics to validate the practicality of the study's implications.

The study concluded that utilizing the BRBF system can yield significant structural cost savings, as high as 34% for a six-story structure, over the use of CBF systems (Dasse, 2009). The savings are the result of both decreased material quantities and lighter foundation demands. Although the BRB members can be more expensive than typical HSS brace sections, the cost is offset by material savings in the columns, beams, connections and the foundation. Also, the generally smaller net area characteristic of the BRB members yield lower connection design forces, which in turn, can result in additional material savings through reduced gusset plate sizes and weld strengths (Dasse, 2009). Shown below is the comparative chart highlighting the savings realized in using the BRBF system for the six-story structure.

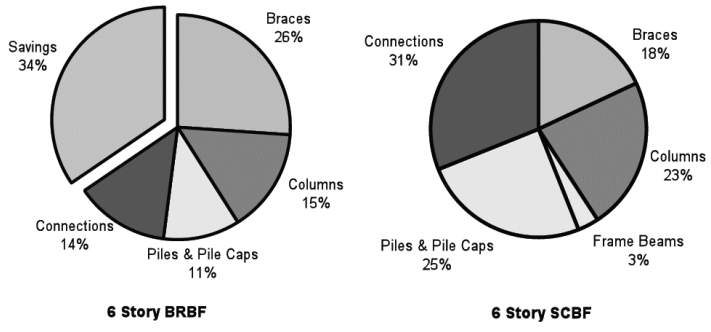


Figure 6.1-1: Relative Costs of the BRBF & CBF for a Six-Story Structure (Dasse, 2009)

Furthermore, the study concluded that the cost savings provided by the use of BRBF systems are more significant as the height of the building increases. The greater quantities of material utilized offset the premium paid for the BRBF members, and also the period and base shear advantages, provided by the BRBF system due to the added ductility, also increase with building height. The graph below shows this positive relationship between cost savings and building height.

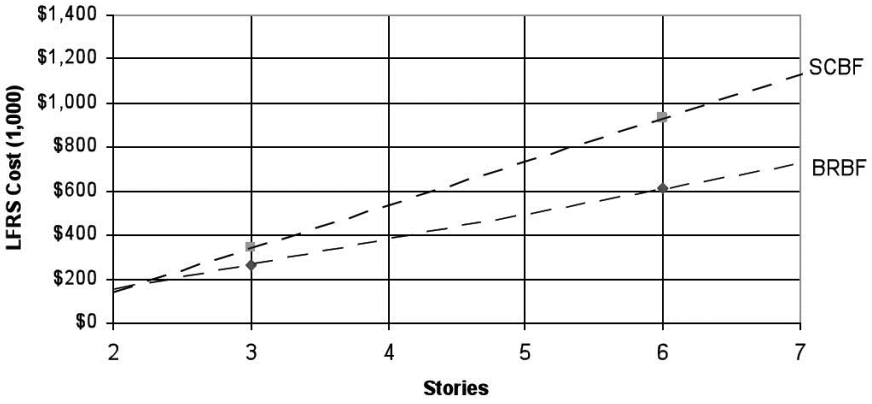


Figure 6.1-2: Lateral Frame Cost as a function of Building Height (Dasse, 2009)

A follow up study was commissioned by StarSeismic™ in the subsequent year to further corroborate their rather bold claims. This time, the analytical study was conducted for design of buildings in a high seismic zone in Europe. Two types of CBF systems were investigated: a low dissipative CBF with very limited ductility and a moderately ductile CBF with dissipative bracing systems, which were then both compared to the BRBF. The conclusions were identical to the previous study: the BRBF, in spite of being more expensive as a brace element, actually leads to significant reductions in total structural costs of buildings in moderate or high earthquake zones by decreasing the required capacity of non-dissipative structural members, as well as reductions in connection requirements (StarSeismic, 2010). The study recapitulated findings from the previous study by Dasse (2009), and is summarized by similar graphs depicting the possible cost savings of utilizing BRBFs over CBFs.

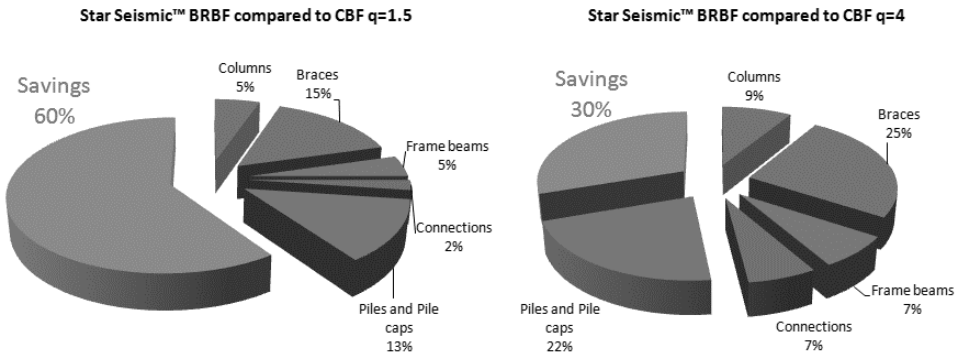


Figure 6.1-3: Relative Cost of the BRBF Compared the CBFs of Different Ductility Capacities (StarSeismic, 2010)

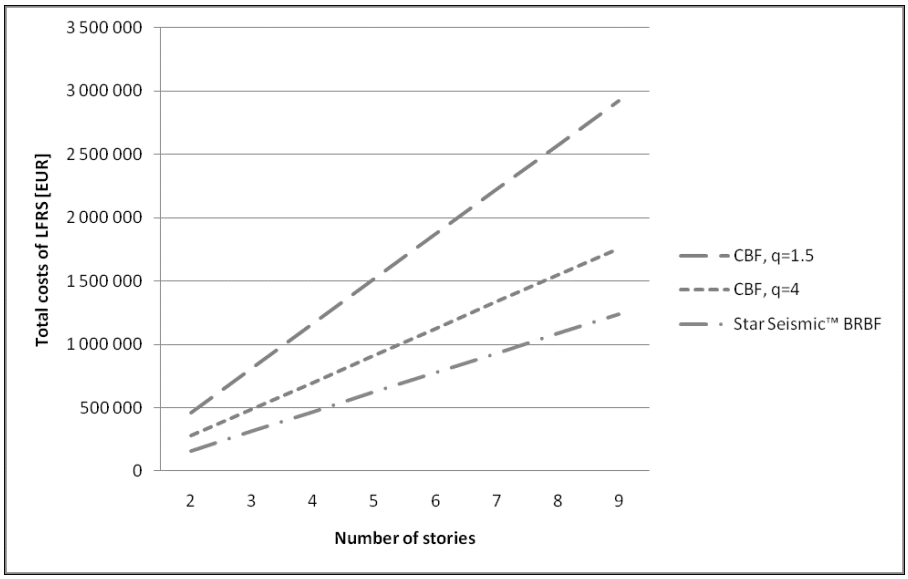


Figure 6.1-4: Lateral Frame Cost as a function of Building Height (StarSeismic, 2010)

The case for the economical advantages of BRBFs over conventional lateral systems has been sufficiently discussed and has also been relatively well-received. There has been a proliferation of BRBF systems being utilized in the design of earthquake-resistant buildings in the West Coast of the United States, in the past decade. A report written by engineers at Arup, the company has used the BRBF system in California on projects comprising of more than four million square feet and totaling more than $1 billion in construction costs to date, as of the year 2003 (Ko and Field, 2003). The use of the BRBF as the primary lateral force resisting system has undeniably gained significant traction in commercial practice, and will only continue to become more prevalent as seismic codes adopt the high-performance brace as a new standard in earthquake-resistant building design.

## 6.2 Self-Centering Energy Dissipating Braces & Hybrid Braces

The economic feasibility of the SCED as well as the HPCD is less well-defined however, and is largely due to the fact that these new developments of high-performance braces simply have not been in existence for a significant period of time. Nonetheless, one study conducted in 2012 by researchers in Italy has attempted to evaluate the cost effectiveness of the SCED as compared to the BRBF and the conventional MRF by a risk-based life cycle cost analysis method (Freddi et al., 2012). The risk-based life cycle cost (LCC) analysis is appropriate in evaluating the cost effectiveness of the different systems throughout the length of the structure's entire life span, from initial construction, maintenance and repair, to deconstruction. The particular importance of repair costs after extreme seismic events is critical in comparing the performance and cost effectiveness of the various high-performance brace systems. The study's findings show that the BRBF is the most cost effective. While the SCED is also cost efficient as compared to the conventional MRF, the expected cost over the life cycle of the building for a SCED system is slightly higher than the BRBF system. Tabulated below is the summary of the findings from the study, which shows the expected cost of each system as a percent of the replacement cost and the loss savings provided by the high-performance braces.

| | **Expected LCC as % of Replacement Cost** | **Loss Savings** |
|---|---|---|
| **MRF** | 309.69 | - |
| **BRBF** | 160.98 | 148.71 |
| **SCED** | 174.50 | 135.19 |

Table 6.2-1: LCC Analysis Results Comparing the MRF, BRBF, and the SCED (Freddi et al., 2012)

# Chapter 7

# Conclusions

*"If we can sort out all the problems today, we wouldn't have to come to work tomorrow, would we." – Peter Rice*

The primary goal of the thesis was to provide useful insights into the current developments of high-performance braces in the hope that such systems can be more widely adopted and utilized by practicing engineers in designing new earthquake-resistant structures. Three different types of high-performance brace systems were presented: (*i*) the buckling-restrained brace frame (BRBF), (*ii*) the self-centering energy dissipating brace frame (SCED), and (*iii)* the hybrid brace frame (HPCD).

The first half of the research included a comprehensive overview on the breadth of available literature regarding the development of high-performance braces. The latter half then

presented the comparative analysis of the various systems to discuss and evaluate the performance implications of high-performance braces, as well as the economic aspects of these new technologies.

Analytical models representing each of the three high-performance brace systems were created for comparison in SAP2000. A control model representing a conventional moment resisting frame was also produced to set the basis for comparison. A nonlinear response history analysis was then performed to evaluate the seismic performance of the high-performance brace systems as measured by parameters such as the peak floor displacements, peak interstory drift ratios, peak interstory residual drift ratios, and peak floor accelerations.

Based on the nonlinear response history analysis, the BRBF and the SCED performed equally best with regards to floor displacements and interstory drift ratios. The HPCD performed better than the SMRF with regards to the same parameters but not as well as the BRBF and the SCED. However, for floor accelerations, the HPCD outperformed all the other systems by a significant margin, as can be explained by the relatively high damping properties of the HDR damper device. Lastly, with regards to the residual drift ratios, the SCED was clearly the best performing system due to its self-centering behavior.

The last chapter discussed the economic aspects of implementing high-performance braces and the possible cost advantages of utilizing these new systems. Case studies were presented to corroborate the claim that using the BRBF over a CBF can result in construction cost savings. As for the SCED and the HPCD, which are very new developments, there did not exist any case studies with empirical data to support their possible cost benefits, as of this writing. Therefore, research conducted in 2012, which used the risk-based life-cycle cost analysis method to calculate the expected savings in replacement costs over the life span of the building by utilizing the BRBF or the SCED, was cited to make the case for the economic practicality of SCED systems. Lastly, since the HPCD is basically a combination of the BRBF with a HDR damper, a device that has been widely prevalent in the field of base isolation mechanisms, the study of its practical implementation was not required. The HPCD would simply be a new application of the HDR damper device, by merging its high-performance characteristics with the BRB.

As with all works of engineering, success does not mean that all the problems have been solved. There are several areas within this thesis that can be further augmented by future research. One possible area for further research can be the scalability of the high-performance braces for implementation in mid to high-rise structures. The performance benefits, as observed in the relatively low-rise structure analyzed in this work, may not be as pronounced or even realized for taller buildings. Another aspect recommended for future research can be a more extensive study of the economic aspects of the high-performance braces, mainly the SCED and the HPCD. As emphasized several times before, the lack of case studies for the two aforementioned brace systems makes it difficult to accurately assess and evaluate the overall effectiveness of utilizing such systems, and in turn, impossible to objectively and confidently recommend the use of these systems.

This work has provided a general overview of the current developments of high-performance braces and an introductory understanding of the possible benefits these new technologies provide in both structural performance and economy. Although it may be overly audacious to claim that the future of designing earthquake-resistant structures will be centered on the use of high-performance braces, the availability of such new technologies only enhances the effectiveness of the structural engineer by providing yet another tool in designing safer and more economical buildings for society.

# References

AlHamaydeh, M., Choudhary, I., & Assaleh, K. (2012). Virtual testing of buckling-restrained braces via nonlinear AutoRegressive eXogenous neural networks. *Journal of Computing in Civil Engineering,* doi:10.1061/(ASCE)CP.1943-5487.0000247

Applied Technology Council (ATC-55 Project). (2005). *FEMA 440 - improvement of nonlinear static seismic analysis procedures* Department of Homeland Security - Federal Emergency Management Agency.

ASCE. (2006). *ASCE/SEI 41-06 Seismic Rehabilitation of Existing Buildings*. Virginia: American Society of Civil Engineers.

ASCE. (2010). *ASCE/SEI 7-10 Minimum Design Loads for Buildings and Other Structures*. Reston, Virginia: American Society of Civil Engineers.

Atlayan, O., & Charney, F. A. (2012). Hybrid buckling-restrained braced frames. *Stessa 2012,* Santiago, Chile. 881.

Bank, R., and Weres, O. (1976). In: Perkins J, editor. Shape memory effects in alloys, NY: Plenum Press.

Black, C., Makris, N., & Aiken, I. (2002). *Component testing, stability analysis and characterization of buckling-restrained unbonded braces.* (Final Report to Nippon Steel Corporation, Tokyo, Japan No. 2002/08). Berkeley, CA: Pacific Earthquake Engineering Research Center.

Budahazy, V. (2012). Modelling of the hysteretic behaviour of buckling restrained braces. *Conference of Junior Researchers in Civil Engineering,* Budapest, Hungary. 34.

Building Seismic Safety Council for the Federal Emergency Management Agency. (2000). *FEMA 356*. Washington, D.C.: National Institute of Building Sciences.

Building Seismic Safety Council for the Federal Emergency Management Agency. (2003). *FEMA 450 - NEHRP recommended provisions for seismic regulations for new*

*buildings and other structures*. Washington, D.C.: National Institute of Building Sciences.

Burkholder, M. (2012). *Performance based analysis of a steel braced frame building with buckling restrained brace.* (MS in Architecture - Architectural Engineering, California Polytechnic State University - San Luis Obispo).

Chandra, R. (2001). "Active shape control of composite blades using shape memory actuation." SMART MATER STRUCT, 10, 1018-1024.

Chao, S., Karki, N., & Sahoo, D. (2012). Seismic behavior of steel buildings with hybrid braced frames. *Journal of Structural Engineering,* doi:10.1061/(ASCE)ST.1943-541X.0000702

Charney, F. A., & Marshall, J. D. (2009). Dynamic response of steel moment-frame structures with hybrid passive control systems. (pp. 1022-1033) American Society of Civil Engineers. doi:doi:10.1061/41084(364)93

Chen, Y. (2010). *Performance of structures with supplemental brace-damper systems.* (Ph.D., University of California, Davis). *ProQuest Dissertations and Theses,* . (520278741).

Cheng, F. Y., Jiang, H., & Lou, K. (2008). *Smart structures : Innovative systems for seismic response control*. Boca Raton: CRC Press/Taylor & Francis Group.

Choi, H., Erochko, J., Christopoulous, C., Tremblay, R. (2008). Comparison of the Seismic Response of Steel Buildings Incorporating Self-Centering Energy Dissipative Braces, Buckling Restrained Braced and Moment Resisting Frames. *World Conference on Earthquake Engineering,* Beijing, China.

Christopoulos, C., Tremblay, R., Kim, H. J., & Lacerte, M. (2008). Self-centering energy dissipative bracing system for the seismic resistance of structures: Development and validation. *Journal of Structural Engineering, 134*, 96.

Christopoulos, C., Tremblay, R., Kim, H., & Lacerte, M. (2008). Self-centering energy dissipative bracing system for the seismic resistance of structures: Development and

validation. *Journal of Structural Engineering, 134*(1), 96-107. doi:10.1061/(ASCE)0733-9445(2008)134:1(96)

Chuang-Sheng, W. Y., Leon, R. T., & DesRoches, R. (2012). Quasi-static and dynamic tests of a smart hybrid brace. (pp. 1610-1619) American Society of Civil Engineers. doi:doi:10.1061/9780784412367.143

Computers and Structures, Inc. (2013). *SAP2000 v11.*

Connor, J. J. (2003). *Introduction to structural motion control*. New Jersey: Pearson Education, Inc.

Darling, S. C., & Eatherton, M. R. (2012). Self-centering truss moment frame with replaceable energy-dissipating elements. *Stessa 2012,* 671.

Dasse Design Inc., Cost Advantages of Buckling-Restrained Braced Frame Buildings, July 2007.

Deulkar, W. N., Modhera, C. D., & Patil, H. S. (2010). Buckling restrained braces for vibration control of building structure. *International Journal of Research and Reviews in Applied Sciences, 4*(4), 363.

Dolce, M., Cardone, D., and Marnetto, R. (2000). "Implementation and testing of passive control devices based on shape memory alloys." EARTHQ ENG STRUCT D, 29, 945-968.

Dusicka, P., & Tinker, J. (2013). Global restraint in ultra-lightweight buckling-restrained braces. *Journal of Composites for Construction, 17*, 139-139-150.

Eberhard, Marc O., and M. A. Sozen. "Behavior-based method to determine design shear in earthquake-resistant walls." *Journal of Structural Engineering*119.2 (1993): 619-640.

Erochko, J., Christopoulos, C., Tremblay, R., & Choi, H. (2011). Residual drift response of SMRFs and BRB frames in steel buildings designed according to ASCE 7-05. *Journal of Structural Engineering,* , 589. doi:10.1061/(ASCE)ST.1943-541X.0000296

Erochko, J., Christopoulos, C., Tremblay, R., & Kim, H. (2013). Shake table testing and numerical simulation of a self-centering energy dissipative braced frame. *Earthquake Engineering & Structural Dynamics,* , n/a-n/a. doi:10.1002/eqe.2290

Fahnestock, L. A., Miller, D. J., & Eatherton, M. R. (2011). Self-centering buckling-restrained braces for advanced seismic performance. (pp. 960-970) American Society of Civil Engineers. doi:doi:10.1061/41171(401)85

Fahnestock, L. A. (2006). *Analytical and large-scale experimental studies of earthquake-resistant buckling-restrained braced frame systems.* (Ph.D., Lehigh University). *ProQuest Dissertations and Theses,* . (305316199).

Freddi, F., Padgett, J.E., Dall'asta, A. (2012). Life-cycle cost analysis of low ductility RC frame buildings retrofitted by modern retrofit techniques. *European Conference on Structural Control 2012,* Genoa, Italy. 92.

Hussain, Saif, Paul Van Benschoten, Mohamed Al Satari, Silian Lin. *Buckling Restrained Braced Frames (BRBF) Structures: Analysis, Design and Approvals Issues*. Coffman Engineers, Inc., Los Angeles, CA, 2005.

International Code Council. (2009). *International building code* IBC.

Kimura K, Yoshioka K, Takeda T, Fukuya Z, Takemoto K. Tests on braces encased by mortar in-filled steel tubes. Summaries of technical papers of annual meeting. Architectural Institute of Japan; 1976. p. 1041– 2

Lopez, W. A., & Sabelli, R. (2004). *Seismic design of buckling-restrained braced frames.* (Steel Tips: Technical Guide).Structural Steel Educational Council.

Marshall, J. D. (2008). *Development, analysis and testing of a hybrid passive control device for seismic protection of framed structures.* (Ph.D., Virginia Polytechnic Institute and State University). *ProQuest Dissertations and Theses,* . (1033236365).

Okazaki, T., & Sherman, J. (2010). Bidirectional loading behavior of buckling-restrained braced frames. (pp. 3548-3559) American Society of Civil Engineers. doi:doi:10.1061/41130(369)320

Pampanin, S., Christopoulos, C., and Priestley, M. J. N. _2003_. "Performance-based seismic response of frame structures including residual deformations. Part II: Multidegree-of-freedom systems." *J. Earthquake Eng.*, 7_1_, 119–147.

PEER, Pacific Earthquake Engineering Research Center. (2013). NGA Database. http://peer.berkeley.edu/nga/

Rezaeian, A., Izadifar, R., & Pirkoohi, S. (2009). Improvement of seismic behavior of concentrically braced frames making use of fuse elements in brace members. *Stessa 2009,* 311.

Ricles, J. M., Sause, R., Gonner, N. P., Chancellor, N. B., & Roke, D. A. (2010). Large-scale experimental studies of damage-free self-centering concentrically-braced frame under seismic loading. (pp. 1498-1509) American Society of Civil Engineers. doi:doi:10.1061/41130(369)136

Ricles, J. M., Sause, R., Gonner, N., & Roke, D. (2009). Design concepts for damage-free seismic-resistant self-centering steel concentrically braced frames. (pp. 1-10) American Society of Civil Engineers. doi:doi:10.1061/41031(341)155

Sabelli, R., Mahin, S., & Chang, C. (2003). Seismic demands on steel braced frame buildings with buckling-restrained braces. *Engineering Structures, 25*, 655.

Sause, R., Ricles, J., Garlock, M. M., Li, J., & Herning, G. (2009). An overview of self-centering steel moment frames. (pp. 1-9) American Society of Civil Engineers. doi:doi:10.1061/41031(341)154

SEAOC Seismology Committee (2009). "Analysis Procedures," May, 2009, *The SEAOC Blue Book: seismic design recommendations*, Structural Engineers Association of California, Sacramento, CA.

Seamer, B. G. (2007). *Evaluation of building code provisions for buckling restrained braced frames using non-linear time history analysis.* (M.S.C.E., California State University, Long Beach). *ProQuest Dissertations and Theses,* . (304710822).

Share, M., Ghalehnovi, M., & Shabakhti, N. (2009). Evaluation of capacity spectrum method for estimate of seismic performance in buckling-restrained braced frame. (pp. 1-10) American Society of Civil Engineers. doi:doi:10.1061/41031(341)305

Skinner, R. I., J. M. Kelly, and A. J. Heine. "Hysteretic dampers for earthquake-resistant structures." *Earthquake Engineering & Structural Dynamics* 3.3 (1974): 287-296.

Sprague, H.O. (2009). Buckling Restrained Brace Frame Application for a Power Plant. *Structures Congress 2009,* 920.

StarSeismic™ Europe Ltd. (2010). *Cost advantages of buckling restrained brace frame buildings in accordance with Eurocode*.

Structural Engineers Association of California. (1995). *Vision 2000: Performance based seismic engineering of buildings*. Sacramento, CA: SEAOC.

Tahmasebi, E., Chancellor, N. B., Ricles, J. M., Sause, R., Akbas, G., & Joo, A. L. (2012). Collapse performance of steel self-centering braced frame systems. *Stessa 2012,* 745.

Tinker, J. A. (2011). *Development of an ultra-lightweight buckling-restrained brace using analytical and numerical methods.* (M.S., Portland State University). *ProQuest Dissertations and Theses, .* (926205091).

Tremblay, R., Lacerte, M., & Christopoulos, C. (2008). Seismic analysis of concentrically braced frame systems with self-centering friction damping braces. *Journal of Structural Engineering, 134*, 108. doi:10.1061/(ASCE)0733-9445(2008)134:1(108)

USGS, United States Geological Survey. (2013). Earthquake Hazards Program. http://earthquake.usgs.gov/

Xie, Q. (2005). State of the art of buckling-restrained braces in asia. *Journal of Constructional Steel Research, 61*, 727.

Ying-Cheng Lin, Choung-Yeol Seo, Ricles, J., & Sause, R. (2009). Earthquake simulations on a self-centering steel moment resisting frame with web friction devices. (pp. 1-10) American Society of Civil Engineers. doi:doi:10.1061/41031(341)149

Yoshino T, Karino Y. Experimental study on shear wall with braces: Part 2. Summaries of technical papers of annual meeting, vol. 11. Architectural Institute of Japan, Structural Engineering Section; 1971. p. 403–4

Zhang, Y., & Hu, X. (2010). Self-centering seismic retrofit scheme for reinforced concrete frame structures: SDOF system study. *Earthquake Engineering and Engineering Vibration, 9*(2), 271-283. doi:http://dx.doi.org.libproxy.mit.edu/10.1007/s11803-010-0012-6

Zhu, S., & Zhang, Y. (2008). Seismic analysis of concentrically braced frame systems with self-centering friction damping braces. *Journal of Structural Engineering, 134*(1), 121-131. doi:10.1061/(ASCE)0733-9445(2008)134:1(121)

Zhu, S., & Zhang, Y. (2008). Performance based seismic design of steel braced frame system with self-centering friction damping brace. (pp. 1-13) American Society of Civil Engineers. doi:doi:10.1061/41000(315)32

# Appendix

## A Ground Acceleration Time History Records

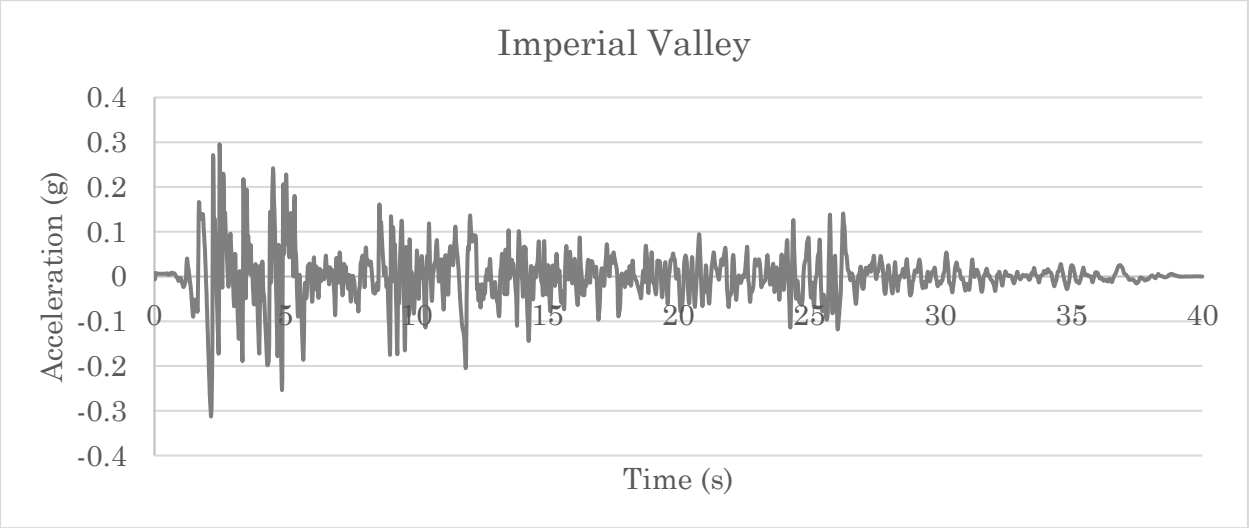


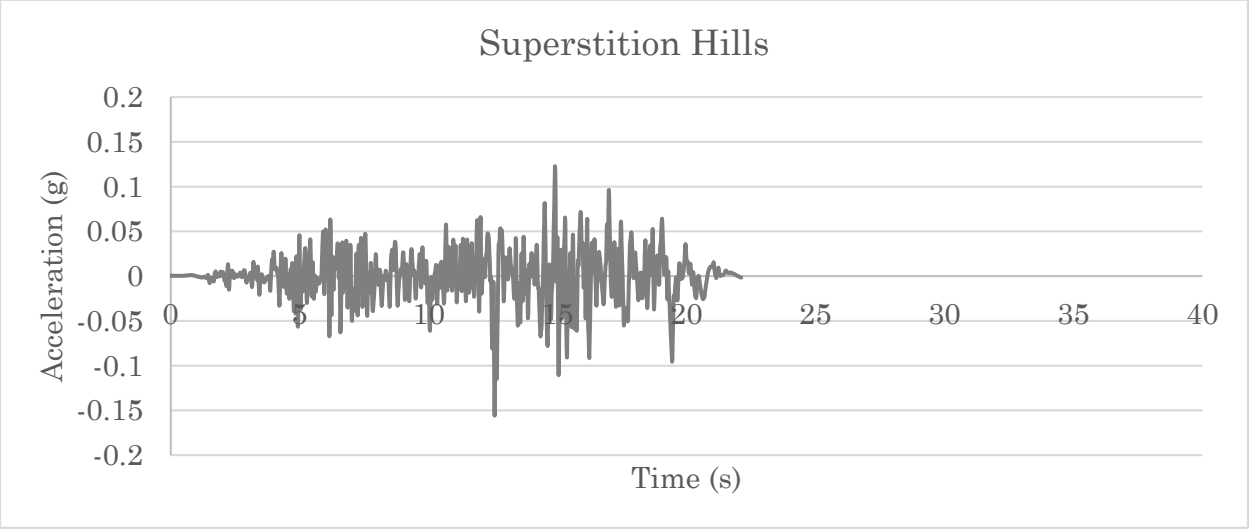

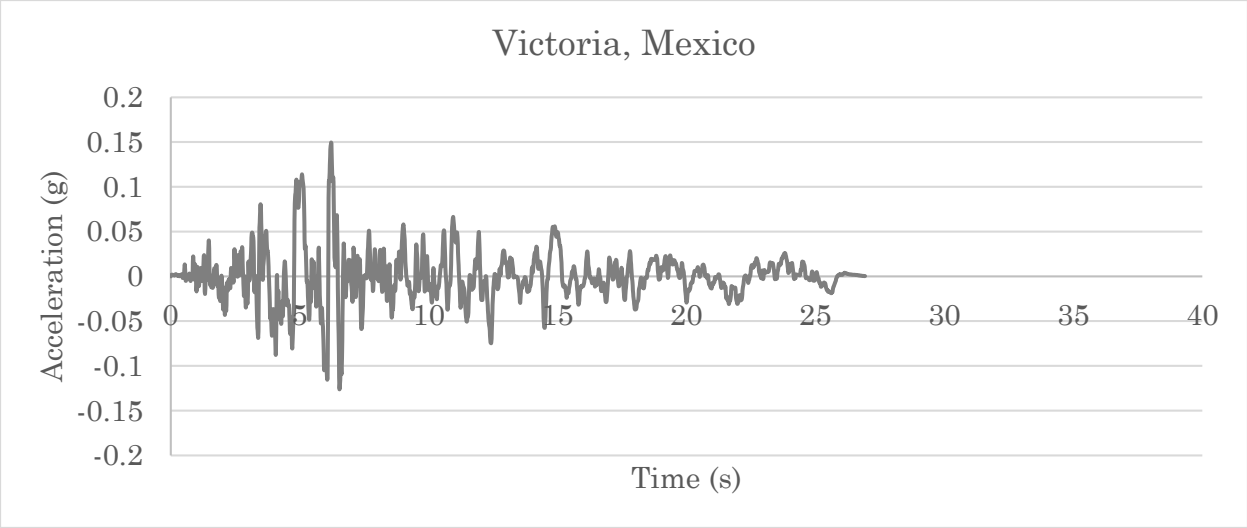
Victoria, Mexico
Acceleration (g)
0.2
0.15
0.1
0.05
0
-0.05
-0.1
-0.15
-0.2
0
5
10
15
20
25
30
35
40
Time (s)


Duzce, Turkey
Acceleration (g)
0.4
0.3
0.2
0.1
0
-0.1
-0.2
-0.3
-0.4
0
5
10
15
20
25
30
35
40
Time (s)

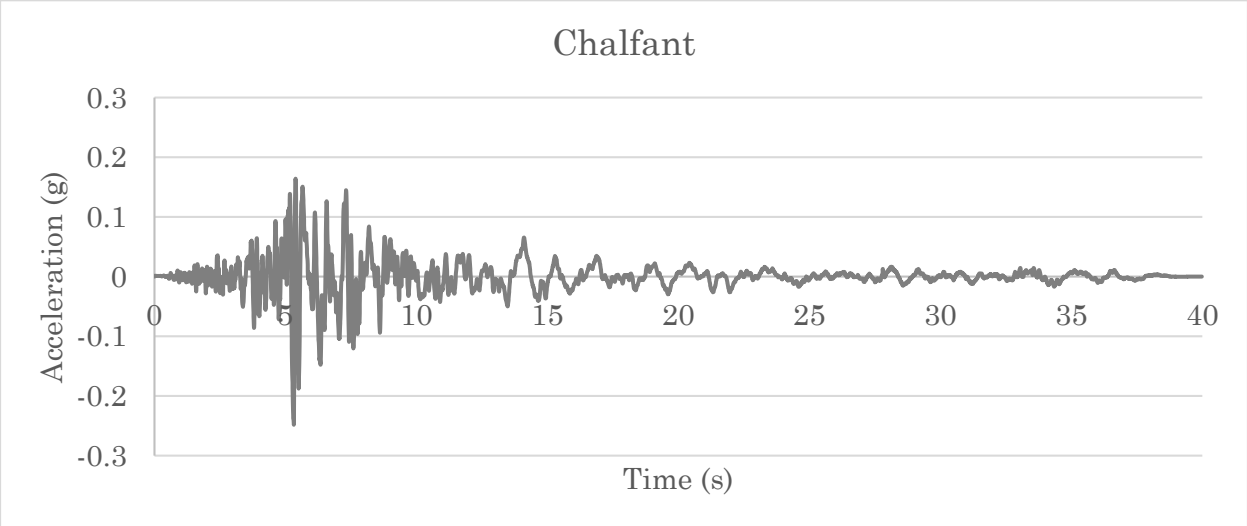
Chalfant
Acceleration (g)
0.3
0.2
0.1
0
-0.1
-0.2
-0.3
0
5
10
15
20
25
30
35
40
Time (s)

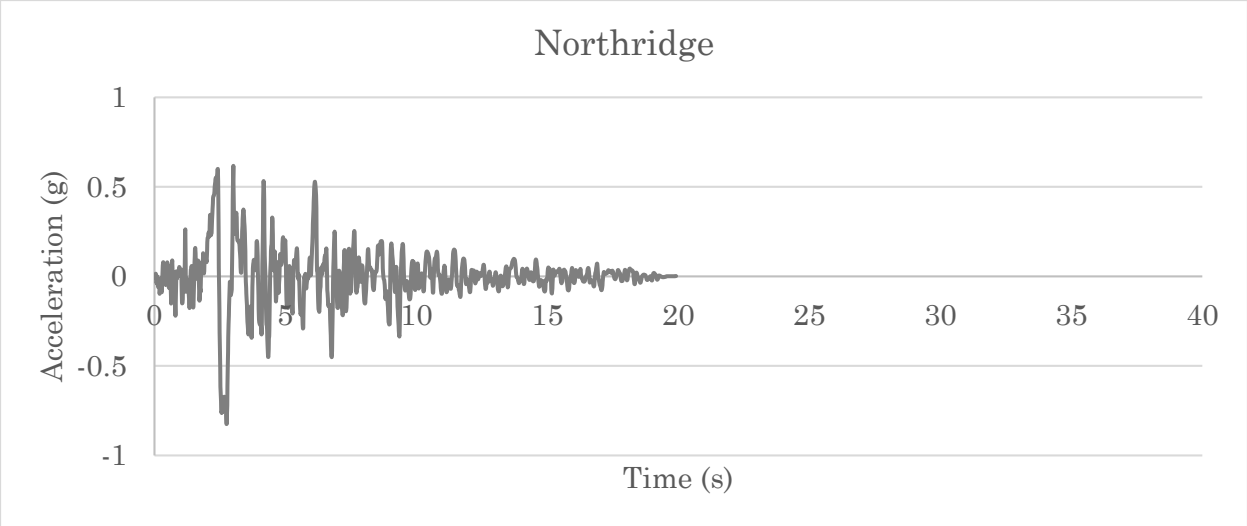
Northridge
Acceleration (g)
1
0.5
0
-0.5
-1
0
5
10
15
20
25
30
35
40
Time (s)

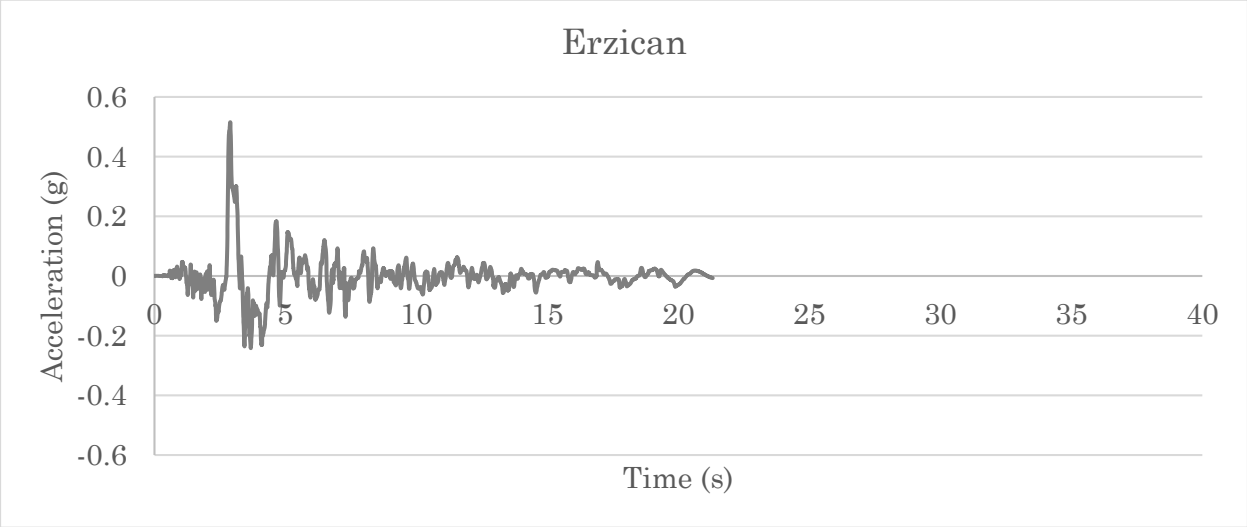
Erzican
Acceleration (g)
0.6
0.4
0.2
0
-0.2
-0.4
-0.6
0
5
10
15
20
25
30
35
40
Time (s)